Errors and uncertainties in regional climate simulations of rainfall variability over Tunisia: a multi-model and multi-member approach

Bilel Fathalli, Benjamin Pohl, Thierry Castel, Mohamed Jomaa Safi

Climate Dynamics (2019) 52:335–361
https://doi.org/10.1007/s00382-018-4150-2

Errors and uncertainties in regional climate simulations of rainfall variability over Tunisia: a multi-model and multi-member approach

Bilel Fathalli[1] · Benjamin Pohl[2] · Thierry Castel[2] · Mohamed Jomâa Safi[1]

Received: 6 June 2017 / Accepted: 13 February 2018 / Published online: 23 February 2018

Abstract
Temporal and spatial variability of rainfall over Tunisia (at 12 km spatial resolution) is analyzed in a multi-year (1992–2011) ten-member ensemble simulation performed using the WRF model, and a sample of regional climate hindcast simulations from Euro-CORDEX. RCM errors and skills are evaluated against a dense network of local rain gauges. Uncertainties arising, on the one hand, from the different model configurations and, on the other hand, from internal variability are furthermore quantified and ranked at different timescales using simple spread metrics. Overall, the WRF simulation shows good skill for simulating spatial patterns of rainfall amounts over Tunisia, marked by strong altitudinal and latitudinal gradients, as well as the rainfall interannual variability, in spite of systematic errors. Mean rainfall biases are wet in both DJF and JJA seasons for the WRF ensemble, while they are dry in winter and wet in summer for most of the used Euro-CORDEX models. The sign of mean annual rainfall biases over Tunisia can also change from one member of the WRF ensemble to another. Skills in regionalizing precipitation over Tunisia are season dependent, with better correlations and weaker biases in winter. Larger inter-member spreads are observed in summer, likely because of (1) an attenuated large-scale control on Mediterranean and Tunisian climate, and (2) a larger contribution of local convective rainfall to the seasonal amounts. Inter-model uncertainties are globally stronger than those attributed to model's internal variability. However, inter-member spreads can be of the same magnitude in summer, emphasizing the important stochastic nature of the summertime rainfall variability over Tunisia.

Keywords Rainfall variability · Tunisia · Uncertainties · WRF ensemble · Euro-CORDEX

1 Introduction

Tunisia, a small country (the northernmost in Africa with a total area of about 164,000 km²) at the junction of the West and East Mediterranean Basin, is considered as one of the most vulnerable Mediterranean countries to climate change and a land of contrasting climate (Verner 2013). It lies in a contact zone marking the transition between the temperate humid Mediterranean climate and the dry Saharan climate. Consequently, the Tunisian climate varies from extremely arid in the south with significant interannual variability in rainfall and severe drought episodes, to a Mediterranean climate in the north with relatively cool, wet winters and warm, dry summers. The central and eastern regions of Tunisia are characterized by a semi-arid climate (Kingumbi et al. 2009) experiencing violent convective storms particularly in summer and autumn (Slimani et al. 2007). Overall, the climate of Tunisia is arid and is directly influenced by the topography, the distance to the sea and the large-scale atmospheric circulation (Berndtsson 1987). Rainfall in Tunisia, indeed, largely depends on the synoptic atmospheric pressure patterns and local orographic features. The rainy season extends from September to May. During this season, rainfall is generally associated with the Polar or the Mediterranean Front given the geographic position of Tunisia in a convergence zone between the tropical maritime and the polar maritime air streams from the Atlantic and its extension eastward (Berndtsson 1989). Northern topographic relief has considerable effects on precipitation through the interception of moist air streams and thus conditioning an overall latitudinal pattern (a north/south general gradient) of the Tunisian rainfall (Slimani et al. 2007; Feki et al. 2012)

✉ Bilel Fathalli
bilelfathalli@yahoo.fr

[1] Université de Tunis El Manar, Ecole Nationale d'Ingénieurs de Tunis, Tunis, Tunisia

[2] Centre de Recherches de Climatologie, UMR6282 Biogéosciences, CNRS/Université de Bourgogne Franche-Comté, Dijon, France

with mean annual totals ranging from more than 1600 mm in the extreme north along the Atlas Mountains thereby denoting a strong orographic forcing, to less than 50 mm on the margins of the Sahara. The amount of rainfall decreases also with increasing distance from the northern Mediterranean coast (Berndtsson 1987). These rainfall gradients integrate, however, a strong spatio-temporal and multi-scale variability (Slimani et al. 2007) marked by a quite complex and heterogeneous topography (mountain ranges in the north, large land depressions in the west central and desert in the south). Local geographic variations can furthermore produce a mosaic of local micro-climates whose characteristics are sometimes very distinct (Slimani et al. 2007).

Although detection of rainfall trends in Tunisia remains very difficult to determine because of a large year-to-year variability, some authors reported that annual rainfall totals have declined by 5% per decade in the north since the 1950s (Verner 2013). Central Tunisia has, nonetheless, experienced since 1989 more extreme rainfall events mainly a significant increase in the number of days with heavy rainfall (> 30 mm) according to Kingumbi et al. (2009). The need for climate information at relatively high resolutions (around 10 km) provided by regional climate models (RCMs) then seems to be necessary in order to examine Tunisian present-day spatio-temporal climate variability. This is of primary importance to study the impacts of climate change on various components of the climate system (water resources, land-use, vegetation, etc.) and to test illustrative scenarios for the future.

However, many studies showed that simulations using RCMs are subject to systematic errors and uncertainties (e.g. Wu et al. 2005; Brown et al. 2013; Syed et al. 2014; Ramarohetra et al. 2015) arising from (1) model configurations (the spatial and temporal resolutions, type of grid, numerical methods, land use databases, etc.: e.g. Tebaldi and Knutti 2007) and that can be evaluated using multi-model ensembles (Holtanova et al. 2014); (2) inaccuracies and uncertainties in the driving lateral conditions that can be transmitted to RCMs (e.g. Duffy et al. 2006; Diaconescu et al. 2007; Sylla et al. 2009); and/or (3) the specific influence of each type of physical parameterizations, that can be assessed in regionalization experiments using a single model with different physical schemes for the same physical process (e.g. Fernandez et al. 2007; Flaounas et al. 2010; Crétat et al. 2011a; Raju et al. 2001). Moreover, a regional climatic signal can be separated to a reproducible fraction associated with external large-scale forcing, and an irreproducible (stochastic) fraction associated with non-linear (chaotic) dynamical and physical processes described by RCM equations. These two components can be separated by using an ensemble of RCM simulations performed under different (identical) initial (boundary) conditions. The reproducible fraction of the climatic signal is characterized by the convergence of the ensemble's members toward similar solution while the irreproducible fraction is characterized by strong inter-member spread and is often referred to as internal variability (e.g., Giorgi and Bi 2000; Christensen et al. 2001; Wu et al. 2005; Alexandru et al. 2007; Lucas-Picher et al. 2008; Crétat et al. 2011b; Wu et al. 2012). The latter can be another source of RCM uncertainties that should be assessed in regional climate studies. Levels of internal variability may be modulated by the synoptic conditions (e.g., Crétat et al. 2011a), the season (e.g., Rinke et al. 2004; Caya and Biner 2004; Sieck et al. 2013; Sanchez-Gomez and Somot 2016), the domain size and location (e.g., Alexandru et al. 2007; Leduc and Laprise 2009; Matsumura et al. 2010) and the model's parameterizations (e.g., Crétat and Pohl 2012).

Many internationally coordinated research programs such as CORDEX (e.g., Ruti et al. 2016 for Med-CORDEX; Kotlarski et al. 2014 for Euro-CORDEX), ENSEMBLES (e.g. Hewitt 2004), and PRUDENCE (e.g., Jacob et al. 2007) are seeking to improve regional climate dynamical and statistical downscaling methods and to better characterize uncertainty in regional climate simulations by comparing and evaluating RCMs outputs for many regions including North Africa. However, few (or none) of these inter-comparison studies, to our knowledge, have attempted to rank and compare the magnitude of uncertainties arising from using different model dynamic configurations and physical parameterizations to those arising from internal variability. This fact then motivates us to raise such an issue in a multi-model and multi-member approach. Hence, we aim in this study to address two major goals.

- First, investigate at different timescales the Tunisian precipitation spatial and temporal variability simulated by a non-hydrostatic limited area model, namely the Weather Research and Forecasting (WRF) model at 12 km spatial resolution, and derived from a set of regional simulations within the Euro-CORDEX framework. We choose to analyze a sample of Euro-CORDEX hindcast regional simulations since they cover Tunisia at ~ 12 km grid spacing and also include simulations performed by the WRF model. RCMs errors and skills in downscaling precipitation variability over Tunisia are, furthermore, assessed by comparison to a local and dense rain gauge network. Many studies using GCM or RCM have investigated the precipitation variability over the Mediterranean Basin (e.g., Xoplaki et al. 2003; Jacob et al. 2007; Lionello et al. 2012; Hertig et al. 2012; Flaounas et al. 2013; Gómez-Navarro et al. (2013, 2015), Kotlarski et al. 2014, Panthou et al. 2016; Cavicchia et al. 2016) or over Africa (e.g., Paeth et al. 2005; Patricola and Cook 2010; Nikulin et al. 2012; Brands et al. 2013; Kim et al. 2014) including Tunisia. Validation of the simulations results over Tunisia is however based on low density observa-

tional networks and/or relatively low resolution global datasets. Indeed the density of the observational network over Tunisia in E-OBS lies only on 13 land based stations (Haylock et al. 2008).

- Second, the present work is supported by a ten-member ensemble of 20 years long simulations (one of the first initiatives to our knowledge) that can enable us to quantify the stochastic (irreproducible) component of the interannual variability of rainfall over Tunisia due to model's internal variability. Inter-member uncertainties are indeed quantified by using simple spared metrics and their magnitude is, furthermore, compared to that of inter-model uncertainties.

The present paper is organized as follows. Section 2 presents the datasets and methods used for this work. Section 3 presents our main results. It first evaluates the skills of a WRF experiment in downscaling precipitation spatial variability over the whole Mediterranean basin. It then thoroughly presents the models skills and uncertainties in regionalizing the mean climate and interannual variability of rainfall over Tunisia. Section 5 finally discusses and summarizes our main results.

2 Data and methods

2.1 Data

2.1.1 Gridded observational datasets

The following precipitation products over the Mediterranean Basin were statistically interpolated onto WRF grids for comparison purposes:

(1) The Climate Research Unit (CRU) high-resolution monthly gridded precipitation dataset version 3.21 (Harris et al. 2014), (2) The University of Delaware (UDEL) monthly global gridded total rain-gauge precipitation datasets version 3.02 (Matsuura and Willmott 2012), (3) the Global Precipitation Climatology Centre (GPCC) Full Data Reanalysis of precipitation version 6 (Schneider et al. 2013).

For validation of the simulated rainfall at finer scales over Tunisia, we use records of a dense rain-gauge network provided by the Tunisian ministry of agriculture. Stations are spread throughout the country with much higher density in the north of the country. Monthly accumulated rainfall is interpolated onto a regular grid using a Thin Plate Splines (TPS) approach. TPS has been widely used to interpolate environmental variables (Li and Heap 2011) such as rainfall data (Tait et al. 2006). The method performs well in comparative studies using other interpolation techniques (Kriging, linear multiple regression, inverse distance weighting: e.g., Hong et al. 2005; Camera et al. 2014; Alvarez et al. 2014) and it is able to account for external variables (e.g., elevation as covariate). As precipitation over Tunisia usually displays a partially varying dependence on topography (e.g., Feki et al. 2012; Slimani et al. 2007), inclusion of elevation data to inform the prediction process reduces prediction errors and gives more precise representations of the higher resolution variability (Hijmans et al. 2005; Tait et al. 2006; Llyod 2010). A trivariate (latitude, longitude and elevation) TPS (based on minimizing the general cross validation) is subsequently performed on a set of 542 rain gauges that have complete and reliable rainfall records over the study period (1992–2011). Elevation is estimated from a digital elevation model (DEM) of Tunisia at 3 km spatial resolution derived from the Shuttle Radar Topography Mission (SRTM, Jarvis et al. 2008) at 3 arc-second (~ 90 m). The scarcity of available records (rain gauges) in the far south of Tunisia leads to some negative values of interpolated precipitation, which are reset to 0 mm.

2.1.2 Satellite remote sensing and blended products

Although satellite precipitation products are subject to some limitations as they cannot pick up local variations in rainfall intensity, have coarse spatial resolution and can underestimate or overestimate rainfall amounts (e.g., Ceccato and Dinku 2010), they are useful for providing rainfall estimates over the seas. The Global Precipitation Climatology Project (GPCP) (Huffman et al. 1997; Adler et al. 2003) and the Tropical Rainfall Measuring Mission (TRMM) 3B42 and 3B43 (Huffman and Bovlin 2017) datasets are then used in this study.

2.1.3 Climate reanalysis

The European Centre for Medium-Range Weather Forecasts (ECMWF) ERA-Interim (ERA-I, hereafter, Dee et al. 2011; Simmons et al. 2007) reanalysis is used to evaluate the WRF-simulated precipitation over the Mediterranean Basin. ERA-I covers the period from 1979 onwards. Its data assimilation and modeling system is based on the Integrated Forecast System (IFS Cy31r2) model. This system includes a 4-dimensional variational analysis (4D-Var) with a 12-h analysis window. ERA-I spatial resolution is approximately 80 km (T255 spectral truncation) on 60 vertical levels from the surface up to 0.1 hPa.

2.1.4 CORDEX RCM hindcast

Precipitation data from 08 regional climate simulations at ~ 12 km spatial resolutions within the Euro-CORDEX framework have been analyzed in this work. Simulations (CLMcom-CCLM, KNMI-RACMO, SMHI-RCA, DHMZ-RegCM, GERICS-REMO, CNRM-ALADIN IPSL-WRF

and UHOH-WRF) are run with 07 regional climate models (Table 1) with different configurations (number of vertical levels, relaxation zone, etc.) and physical parameterizations, but all using the 6-hourly ERA-I reanalysis for lateral forcing. A more detailed description of the Euro-CORDEX simulations can be found in Vautard et al. 2013 or Kotlarski et al. 2014. All simulations were regridded and projected into the WRF grid for grid-cell-by-grid-cell comparisons.

2.2 Setup of the WRF ensemble

The set of numerical experiments in this study consists of a 10-member ensemble of regional simulations performed using the non-hydrostatic Weather Research and Forecasting/Advanced Research WRF (ARW) model (Skamarock et al. 2008) in its version 3.3.1 (CRC-WRF hereafter). WRF is an atmospheric simulation system with a growing user community, offering a large number of physical parameterizations, and suitable for use in a broad range of applications across scales ranging from meters to thousands of kilometers. Two two-way nested domains of 120×60 and 46×71 grid points were used at respectively 60 and 12 km horizontal resolution. The two domains have 28 vertical levels between the surface and 50 hPa. The outer domain (Fig. 1a) covers the Mediterranean basin, including Southern Europe and North Africa, allowing the regional model to develop small-scale features in the simulated synoptic and mesoscale circulations. The second domain is centered on Tunisia. Due to the prohibitive computation costs, our second domain is unfortunately not covering the whole Tunisia as it is very close to the Tunisian land boundaries and slightly cuts the southeastern border of the country.

The chosen physical parameterizations include the WRF Single Moment 6-class (WSM6, Hong and Lim 2006) cloud microphysics, the Yonsei University parametrization of the Planetary Boundary Layer (PBL) by Hong et al. (2006), the Rapid Radiative Transfer Model (RRTM) scheme (Mlawer et al. 1997) for longwave and the Dudhia (1989) scheme for shortwave radiation. The Kain–Fritsch scheme (Kain 2004) is used to parameterize atmospheric convection over the two domains. Over the continents, WRF is coupled with the 4-layer Noah land surface model (Chen and Dudhia 2001). Surface data is derived from the 20-category Moderate Resolution Imaging Spectroradiometer (MODIS) land use data with inland water bodies (Friedl et al. 2002). The initial and lateral boundary conditions for the outer domain are obtained from ERA-I. Lateral forcings are provided every 6 h at a 0.75° horizontal resolution and 19 pressure levels. No nudging technique is applied but only a buffer zone composed of five grid points (1-point specified zone and 4-point relaxation zone) is specified on the periphery of each domain allowing for a smooth transition between the model's prognostic variables and the driving reanalysis, and between the parent and nested grids. The buffer zone (Fig. 1a) was excluded when analyzing the simulation over the Mediterranean Domain. An analysis domain was also defined over Tunisia (Fig. 1a) by discarding from domain #2 the peripheral zone where the jump of resolution between the parent and nested domains leads to spurious values of precipitation. Sea Surface Temperature (SST) fields are prescribed every 24 h by linear interpolation of monthly ERA-I SSTs. The GHG concentrations are constant throughout the simulation.

Following Alexandru et al. (2007), Lucas-Picher et al. (2008) or Sanchez-Gomez and Somot (2016), all members of the WRF ensemble share exactly the same experimental setup (same physical parameterizations and time-dependent lateral boundaries conditions) but differ in their atmospheric initial conditions, perturbed by only modifying the model initialization time (from January 1st, 1991, at 0 h UTC to January 3rd at 18 h UTC, every 6 h). Integration for each member extends over 21 (1991–2011) years with

Table 1 Main characteristics of the used Euro-Cordex simulations

Model	Institution	Label	Resolution	Length of the run	References
ALADIN 5.3	Centre National de Recherches Météorologiques (CNRM)	CNRM-ALADIN	0.11°	1989–2008	Bénard et al. (2010)
CCLM 4.8.17	CLM Community (CLMcom)	CLMcom-CCLM	0.11°	1989–2008	Rockel et al. (2008)
RACMO 2.2	Royal Netherlands Meteorological Institute (KNMI)	KNMI-RACMO	0.11°	1979–2012	Meijgaard van et al. (2012)
RCA 4	Swedish Meteorological and Hydrological Institute (SMHI)	SMHI-RCA	0.11°	1979–2010	Kupiainen et al. (2011)
RegCM 4.2	Državni hidrometeorološki zavod (DHMZ)	DHMZ-RegCM	0.11°	1989–2008	Giorgi et al. (2012)
REMO 2009	Climate Service Center Germany (GERICS)	GERICS-REMO	0.11°	1989–2008	Jacob et al. (2012)
WRF 3.3.1	Institut Pierre Simon Laplace/Institut National de l'Environnement Industriel et des Risques (IPSL-INERIS)	IPSL-WRF	0.11°	1989–2008	Skamarock et al. (2008)
WRF 3.3.1	University of Hohenheim (UHOH)	UHOH-WRF	0.11°	1989–2009	Skamarock et al. (2008)

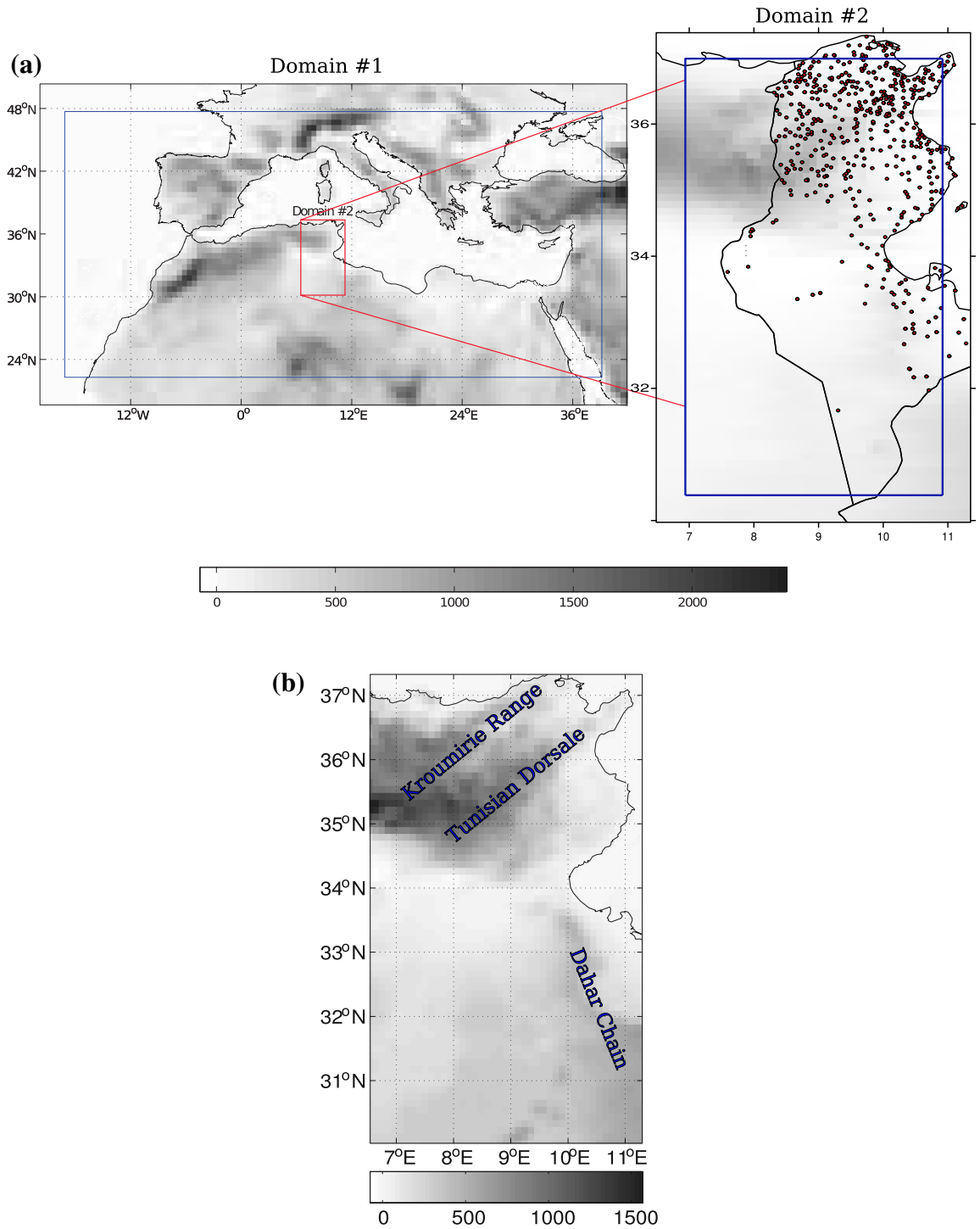

Fig. 1 **a** Presentation of the WRF domains. Shadings represent the topography such as it appears in WRF grids at a 60 km horizontal resolution (domain #1: Mediterranean Basin) and 12 km resolution (domain #2: Tunisia). Rain gauge stations are located within domain #2. Analyzed domains (see text for details) are marked by blue frames. **b** Topography of Tunisia showing the main mountain ranges cited in the text

the first year being discarded for spin-up. Other methods can be used for generating an RCM ensemble like adding random or fixed perturbations in some of the atmospheric fields (Lucas-Picher et al. 2008). However, the source or the magnitude of the perturbations seems to have no impact on the level of internal variability few days after the initiation of the simulations, according to Lucas-Picher et al. (2008) and Giorgi and Bi (2000).

2.3 Evaluation of the regional simulations and ranking of uncertainties

The efficiency of the WRF ensemble, ERA-I and of a sample of Euro-CORDEX regional simulations in simulating the precipitation variability over Tunisia is addressed through comparisons to rain gauges data. Comparisons and computations (i.e. averaged statistics, averaged rainfall amounts and daily indexes, etc.) are made for the grid points inside the analysis domain (defined in Sect. 2.2) and within Tunisia i.e. after applying a mask to exclude the grid points within Algeria and Libya. Comparisons are also made for the common period between the WRF ensemble and the used Euro-CORDEX simulations (1992–2008). Current verifications metrics are used: Mean Bias Error (MBE), Root Mean Square Error (RMSE), Pearson correlation coefficient and graphically normalized Taylor Diagrams (Taylor 2001) which provide quantitative assessment of the spatial variability of precipitation compared to observational data (Bosilovich et al. 2008). The degree of spatial matching between simulations and surface precipitation data estimates is also evaluated by plotting the precipitation empirical cumulative distribution functions (CDF) and then comparing these distributions using the Kolmogorov–Smirnov (KS) statistic test (Darling 1957). The KS test allows a non-parametric measure of distances as it is computed from the maximum difference between two empirical cumulative distribution functions. KS can be defined as:

$$KS = max\left|CDF_{obs}(x) - CDF_{mod}(x)\right|. \quad (1)$$

The null hypothesis (H_0) is that the two samples are from the same continuous distribution. The alternative hypothesis is that they are from different continuous distributions. The critical values for the KS statistic are obtained by a bootstrap procedure (Bargaoui et al. 2013).

Inter-member and inter-model spreads are ranked using the inter-member (or the inter-model) standard deviation which can be written according to Alexandru et al. (2007) or Lucas-Picher et al. (2008) as:

$$\sqrt{\sigma_P^2(\mathrm{i,j,t})} = \sqrt{\frac{1}{M-1}\sum_{\mathrm{m}=1}^{M}\left(P(\mathrm{i,j,t},m) - \bar{P}(\mathrm{i,j,t})\right)^2}, \quad (2)$$

where $\sigma_P^2(i,j,t)$ is the inter-model or the inter-member variance which allows to quantify the spread among the used ensemble of Euro-CORDEX models or among the WRF ensemble members (also model's internal variability). P (*i, j, t, m*) is the value of surface precipitation (annual, DJF, JJA and daily totals) at a position (*i, j*) within the grid at the time *t* and for the member (or Euro-CORDEX simulation) *m* among the total number *M* of members of the ensemble (M = 10) (or used Euro-CORDEX simulations) and $\bar{P}$ (*i, j, t*) is the WRF ensemble mean (or mean of all used Euro-CORDEX simulations) defined as:

$$\bar{P}(i,j,t) = \frac{1}{M}\sum_{m=1}^{M} P(i,j,t,m). \quad (3)$$

Spatial distribution of internal variability can be estimated by computing for each grid point the time-averaged $\sigma^2{}_{\mathrm{p}}$ defined as:

$$\overline{\sigma_P^2}^{t}(i,j) = \frac{1}{N}\sum_{t=1}^{N}\sigma_P^2(i,j,t), \quad (4)$$

where N is the number of time steps over the study period (based on the archival interval of 24 h), while its temporal evolution is given by the spatially averaged of $\sigma^2{}_{\mathrm{p}}$ computed as:

$$\overline{\sigma_P^2}^{ij}(t) = \frac{1}{IxJ}\sum_{i=1}^{I}\sum_{j=1}^{J}\sigma_P^2(i,j,t), \quad (5)$$

where I and J are the number of grid cells in the horizontal x- and y-directions over the domain. The space–time averaged inter-member (or inter-model) variance is then defined as:

$$\overline{\sigma_P^2}^{t,ij} = \frac{1}{N}\sum_{t=1}^{N}\overline{\sigma^2}^{\mathrm{ij}}{}_P(t). \quad (6)$$

Uncertainties due to internal variability and to differences in model configuration choices are then ranked by computing the ratio between the space–time averaged inter-member and inter-model standard deviations.

Following Crétat et al. (2011a, b) we also quantified the reproducibility of precipitation variability between the WRF ensemble members (i.e. the fraction of climate signal that is reproducible from one member to another) by computing for each grid point the ratio (*f*) between the annual variance of all members of the WRF ensemble (20 years/seasons duplicated 10 times) σ_m^2 and that of the ensemble mean (20 years/seasons) $\sigma_{\bar{P}}^2$. The f-ratio is then defined as:

$$f = \frac{\sigma_{\bar{P}}^2}{\sigma_m^2}. \quad (7)$$

3 Results

3.1 Precipitation in the Mediterranean Basin

We first start by giving a quick overview about the WRF simulation skills in downscaling precipitation spatial

variability over the Mediterranean Basin at 60 km spatial resolution. The long-term WRF (ensemble mean) annual precipitation biases (relative biases in percentage) against ERA-I, and against observational datasets (GPCP, TRMM, CRU, GPCC and UDEL) are shown in Fig. 2. ERA-I is also compared to the same references in order to quantify the magnitude of the WRF errors compared to its driving model (i.e. to know wherever WRF improves or degrades the precipitation field of the driver). At the scale of the whole domain, WRF produces dry biases whatever the dataset used as reference. Wet biases over the continent generally show spatial patterns superimposed with the orography (except for CRU), the model probably responding too strongly to the orographic forcing and simulating therefore too marked altitudinal gradients. Wet biases against ERA-I prevail in coastal North Africa, and over the seas. Dry biases are however prevalent south of the domain, and in western Mediterranean Sea against TRMM. ERA-I biases are overall less intense, correlation coefficients between ERA-I and the comparing references are slightly higher than for WRF (Table 2). The later does not seem to improve upon its global driver model. Furthermore, the major ERA-I biases spatial signatures (like the longitudinal wet bias south of the domain against CRU) are globally reproduced by WRF but more intensively. Mean seasonal WRF and ERA-I biases against GPCP are also shown in Table 2 showing better performance for ERA-I especially in summer.

The mean annual cycle of the simulated monthly rainfall and the comparing observational datasets are shown in Fig. 3. Over landmasses, the strong seasonality of the Mediterranean precipitation and its unimodal distribution showing a rainfall peak recorded in winter are well captured in the WRF ensemble simulation despite a minor timing shift (Fig. 3a) concerning the precipitation minimum occurrence. Indeed, the precipitation minimum in all continental datasets is recorded in July while it exclusively occurs in August in the WRF experiment. TRMM and GPCP always show systematically higher rainfall amounts compared to the other datasets. the WRF simulated rainfall mean annual cycle over landmasses is, furthermore, in good agreement with GPCC, CRU and UDEL during the first half of the year. However, the model unlike ERA-I significantly underestimates precipitation from June to December (more intensively from July to October). Temporal correlation coefficients averaged over landmasses are furthermore generally higher for ERA-I (e.g., $R = 0.97$ against GPCC) than for WRF (e.g., $R = 0.9$ against GPCC).

Over the seas (Fig. 3b), the WRF timing error against observation is corrected. Moreover, the WRF ensemble mean perfectly agrees with ERA-I when simulating the summertime rainfall unlike the model does in the other seasons. However, both ERA-I and WRF underestimate the mean annual cycle of rainfall with regard to GPCP and TRMM.

3.2 Precipitation in Tunisia

Does the 12 km grid spacing nested domain captures the main features of rainfall variability over Tunisia (second simulation domain)? How do the uncertainties between the ten members of the WRF ensemble compare to those of a sample of Euro-CORDEX models that differ in many aspects? To address these two questions, we present in the remainder of this study the results of WRF downscaling experiments over Tunisia and of 8 Euro-CORDEX simulations. The simulated precipitation is here evaluated against a dense network of in situ monthly observations.

3.2.1 Mean climate

The climatological (1992–2011) annual and seasonal WRF ensemble mean (WRF_Ens, hereafter) precipitation amounts over Tunisia are shown in Fig. 4. Mean spatial patterns of annual precipitation show a clear latitudinal gradient (decreasing rainfall towards the south), with mean annual totals ranging from a maximum of nearly 760 mm/year in the north to less than 20 mm/year on the margins of the Sahara (Grand Erg Oriental). The orographic maximum is observed in the far north of Tunisia along the Kroumirie mountain range (peaking at Djebel Chambi, 1544 m), which forms one of the wettest regions of North Africa (Fig. 1b). This rainfall gradient prevails throughout the year, albeit time-dependent amplitudes (6–290 mm/season in winter versus 0–71 mm/season in summer), in agreement with Slimani et al. (2007). Spatially averaged seasonal amounts are however rather close from one season to another except in summer (Fig. 4).

Figures 5a, 6a respectively show the WRF_Ens, ERA-I and 08 Euro-CORDEX regional simulations, annual and JJA mean relative biases (MBE in percentage) against a 20-year-high resolution monthly gridded precipitation dataset derived from national rain gauge records. Spatial patterns of the DJF biases are nonetheless roughly similar to those observed for the annual biases and then are not shown. The grid points for which observed rainfall amounts are set to zero mm are then left blank on these maps. Spatial distribution of WRF_Ens annual biases shows that the model overestimates rainfall along the Tunisian Dorsale [a southwest-northeast trending mountain range that mostly constitutes the eastern end of the Atlas Mountain and runs across Tunisia from the Algerian border in the west to the Cap Bon Peninsula in the east (Fig. 1b)], in central (salt land depressions) and southern Tunisia [the low sandstone Dahar mountain chain (Fig. 1b)]. It mainly underestimates annual totals along the neighboring Algerian Atlas and the Kroumirie range. Space–time averaged WRF_Ens biases (Table 3) are dry for the annual rainfall amounts (− 1.6%) while they are wet in DJF (~5%) and mainly in JJA (~30%) totals. WRF_Ens is broadly in good agreement with the driving ERA-I reanalysis especially in

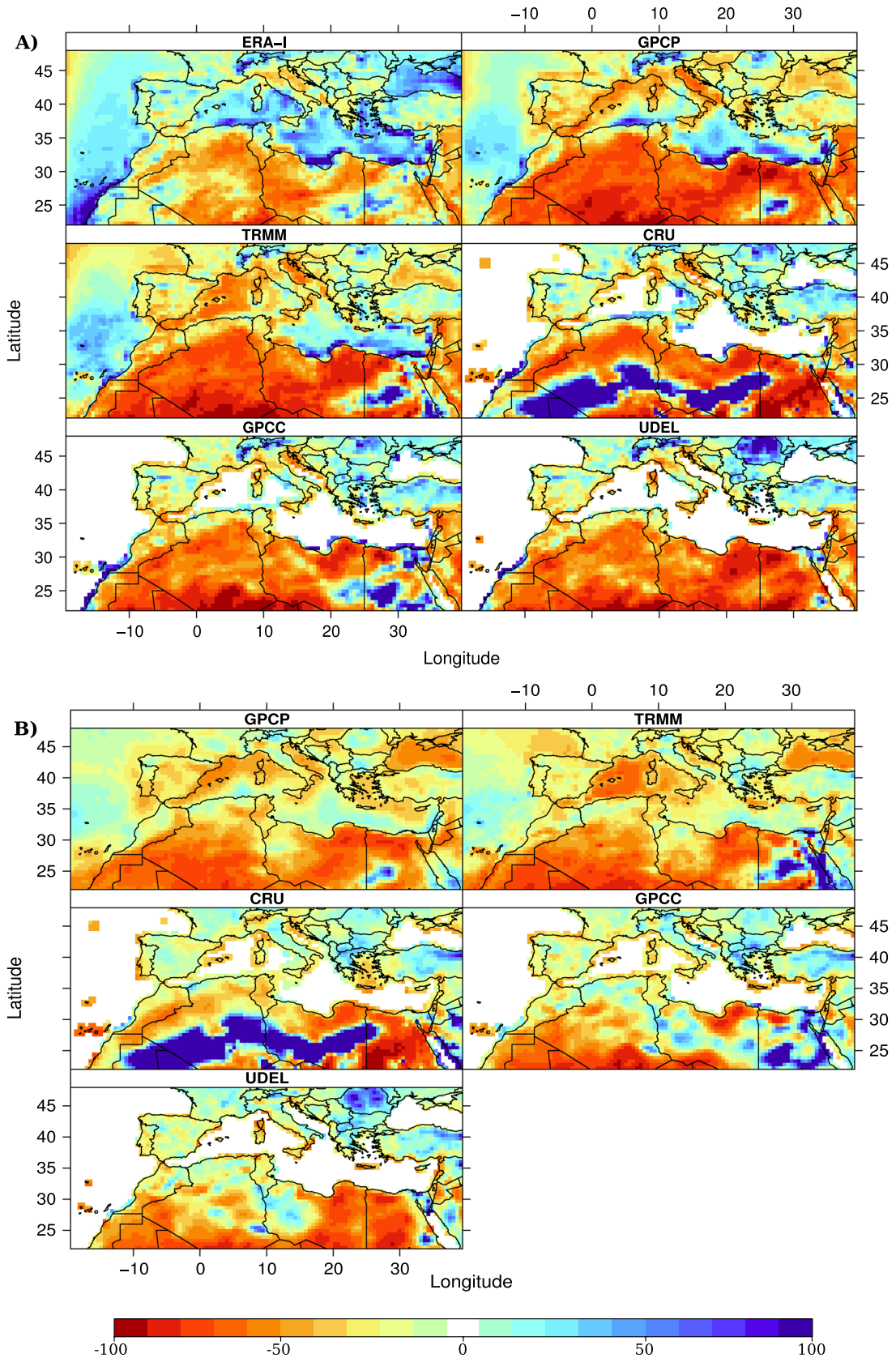
A)
ERA–I
GPCP
TRMM
CRU
GPCC
UDEL
Latitude
Longitude
B)
GPCP
TRMM
CRU
GPCC
UDEL
Latitude
Longitude
-100
-50
0
50
100

◂**Fig. 2** **a** Annual mean WRF (ensemble mean) biases (in percentage) over the Mediterranean analyzed domain (see text for definition) and against ERA-I (period: 1992–2011), GPCC (period: 1992–2010), GPCP (period: 1996–2010), TRMM (period: 1998–2010), CRU (period: 1992–2011) and UDEL (period: 1992–2010). **b** Annual mean ERA-I biases (in percentage) against the same reference datasets

DJF even though ERA-I shows a slightly higher mean spatial correlation coefficient value against observational data. WRF_Ens biases in JJA show rather a different pattern since wet biases are almost prevalent throughout the country. Contrary to DJF, the model is best reproducing the spatial distribution of JJA observed precipitation with the highest spatial correlation coefficient (R = 0.89), so WRF, at finer scale, seems to better capture the summer precipitation spatial variability than the driver does.

With regard to the Euro-CORDEX simulations results for Tunisia, spatial patterns of rainfall biases also show a quite seasonal dependency. While spatial distributions of models relative biases are almost comparable in DJF (not shown), JJA spatial patterns of biases show important inter-model discrepancies and even more clear for the simulations performed with the same model (CRC-WRF, IPSL-WRF and UHOH-WRF). Space-time averaged biases in DJF are dry for most of Euro-CORDEX simulations (excepting DHMZ-RegCM, KNMI-RACMO and SMHI-RCA, Table 3). Averaged biases in JJA are however wet especially for UHOH-WRF and DHMZ-RegCM and excepting the CLMcom-CCLM, GERICS-REMO and KNMI-RACMO simulations (Table 3). The largest space-time averaged RMSE values are otherwise recorded by DHMZ-RegCM in both DJF and JJA seasons (Table 3). This DJF (JJA) high (low) similarity between regional simulations also concerns the members of the WRF ensemble. Figures 5b, 6b show indeed for each grid point the percentage of individual members biases against observation that agree with the ensemble mean (i.e. sharing the same bias sign with the ensemble mean) and thus reflect the reproducibility of errors from one member to another. Results show that the highest mean percentages of reproducibility are obtained for the mean annual and DJF (not shown) totals (respectively ~ 93 and ~ 97%) unlike in JJA (~ 82%) when members are less in agreement with their ensemble mean and so low percentages of reproducibility (30%) can be notably observed north of Tunisia. We furthermore compare in Table 4 the inter-member and inter-model uncertainties by computing the space–time averaged inter-member and inter-model standard deviations (based on Eq. 6) of the rainfall totals, as well as the ratio between these two metrics. Table 4 then shows that inter-model spreads are stronger, at both annual and DJF timescales, than uncertainties due to small changes in the initial conditions of the WRF experiment. Inter-member standard deviation is however equal to the inter-model standard deviation in JJA despite the low amounts of rainfall, and consistently with our previous findings, the ratio between the two spread metrics is also strongest in JJA insinuating the importance of summer inter-member spreads.

Figure 7 summarizes the skills of the WRF experiment, ERA-I and the used sample of Euro-CORDEX regional simulations in simulating the observed spatial mean annual and seasonal (DJF and JJA) precipitation totals over Tunisia. Normalized spatial Taylor diagrams (Fig. 7a), spatial CDFs of observational data and RCM data (Fig. 7b) as well the differences (i.e. distances) between the space-averaged observed and simulated precipitation distributions evaluated with the KS test (Fig. 7c) all confirm the season-dependency of RCM skills and models spreads. The KS scores are below the critical value at the 5% level (the horizontal red lines in Fig. 8c) (i.e. simulations and observation data are from the same continuous distribution) for ERA-I, UHOH-WRF, SMHI-RCA, CLMcom-CCLM and WRF_Ens. in DJF and only for CNRM-ALADIN and WRF-UHOH in JJA. CLMcom-CCLM simulation is however farthest from the observation in JJA. A larger spread of WRF members (Fig. 7a, b) is notable in JJA unlike DJF when members are practically indistinguishable. Note also that the occurrence frequency of annual and DJF (JJA) rainfall below 0.5 (0.1) mm/day in CNRM-ALADIN and DHMZ-RegCM is equal to zero.

Mean annual cycles of observed and simulated rainfall in Tunisia are depicted in Fig. 8a. Observed rainfall shows a unimodal distribution with a maximum in winter (January: ~ 1.2 mm/day) and a minimum in summer (July: ~ 0.1 mm/day). This timing, unlike the Mediterranean Basin, is in agreement with WRF_Ens. The latter is also very close to ERA-I and to observation when simulating the summer dryness, in spite of a rather large spread between members. With comparison to the other Euro-CORDEX simulations, DHMZ-RegCM notably overestimates rainfall amounts particularly in JJA and SON unlike most of the other simulations especially CLMcom-CCLM, which systematically underestimates rainfall all over the annual cycle. IPSL-WRF and UHOH-WRF are moreover particularly wet during summer. Temporal correlation coefficients averaged over the annual cycle are highest for KNMI-RACMO (0.92), very high for WRF_Ens (0.90) while rank between 0.63 and 0.88 for the other used regional simulations.

3.2.2 Interannual variability

Interannual variability of observed and simulated annual, DJF and JJA rainfall totals in Tunisia are respectively given in Fig. 8b–d. The main features of Tunisian rainfall variability are well simulated in the WRF experiment, in spite of time-varying biases. The WRF_Ens interannual bias ranks indeed between − 37 and 17% for the annual totals while it ranks between − 42 to 51% in DJF and − 79% to 80% in JJA. Concerning the Euro-CORDEX multi-RCM hindcast, skills

Table 2 Space–time averaged WRF members (min, max and mean values), and ERA-I annual (and seasonal) simulated rainfall errors and spatial correlations against GPCC, CRU, UDEL, GPCP and TRMM (against GPCP)

Reference dataset	Simulation					
	WRF ensemble			ERA-I		
	MBE (%)	RMSE (%)	R	MBE (%)	RMSE (%)	R
Annual						
ERA-I	Min: − 4.11	Min: 35.00	Min: 0.94			
	Max: − 2.67	Max: 36.41	Max: 0.95			
	Ens. mean: − 2.80	Ens. mean: 35.38	Ens. mean: 0.94			
GPCC	Min: − 19.88	Min: 40.88	Min: 0.92	− 11.93	32.21	0.95
	Max: − 17.45	Max: 41.90	Max: 0.93			
	Ens. mean: − 18.59	Ens. mean: 41.42	Ens. mean: 0.92			
CRU	Min: − 10.39	Min: 45.54	Min: 0.92	− 3.65	42.25	0.95
	Max: − 8.16	Max: 46.34	Max: 0.93			
	Ens. mean: − 9.3	Ens. mean: 45.87	Ens. mean: 0.92			
UDEL	Min: − 23.26	Min: 42.51	Min: 0.90	− 15.37	33.15	0.94
	Max: − 21.16	Max: 43.30	Max: 0.91			
	Ens. mean: − 22.22	Ens. mean: 42.71	Ens. mean: 0.90			
GPCP	Min: − 30.12	Min: 47.78	Min: 0.90	− 30.02	38.87	0.94
	Max : − 28.30	Max: 49.21	Max: 0.90			
	Ens. mean: − 29.23	Ens. mean: 48.36	Ens. mean: 0.90			
TRMM	Min: − 28.34	Min: 47.01	Min: 0.90	− 26.84	40.01	0.93
	Max: − 26.33	Max: 48.17	Max: 0.91			
	Ens. mean : − 27.31	Ens. mean: 47.51	Ens. mean: 0.91			
DJF						
GPCP	Min: − 26.33	Min: 49.84	Min: 0.89	− 32.33	42.71	0.93
	Max: − 26.15	Max: 50. 42	Max: 0.89			
	Ens. mean: − 26.25	Ens. mean: 50.16	Ens. mean: 0.89			
JJA						
GPCP	Min: − 36.40	Min: 68.43	Min: 0.81	− 32.84	55.21	0.93
	Max: − 41.11	Max: 71.14	Max: 0.83			
	Ens. mean: − 38.85	Ens. mean: 69.45	Ens. mean: 0.82			

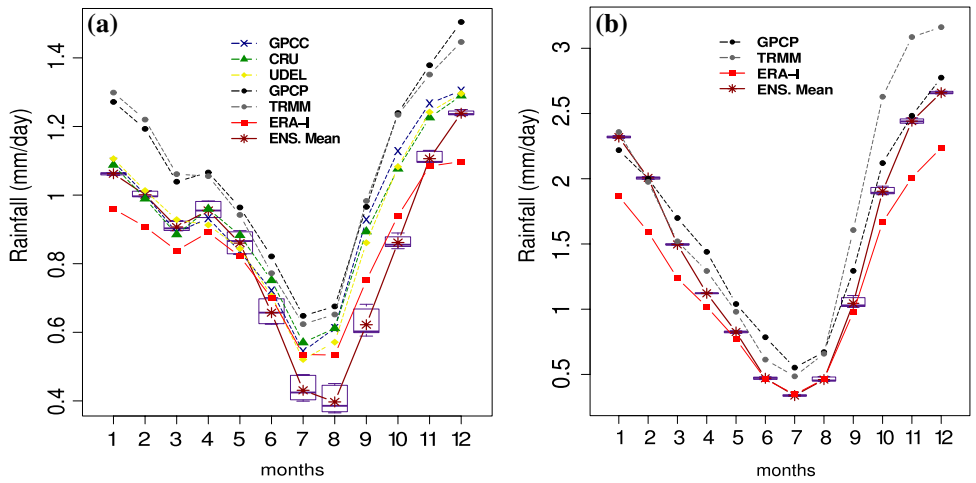

Fig. 3 **a** Rainfall (mm/day) annual cycle averaged spatially over the landmass grid-points of the Mediterranean analyzed domain, and according to ERA-I, several reference datasets and the WRF ensemble. The WRF ensemble mean is represented as a solid curve and individual members are represented as box-and-whisker plots. The boxes have lines at the lower quartile, median and upper quartile values, the whiskers are lines extending from each end of the box to show the range of the data. **b** As **a** but for the sea surfaces according to ERA-I, GPCP, TRMM and the same WRF simulations

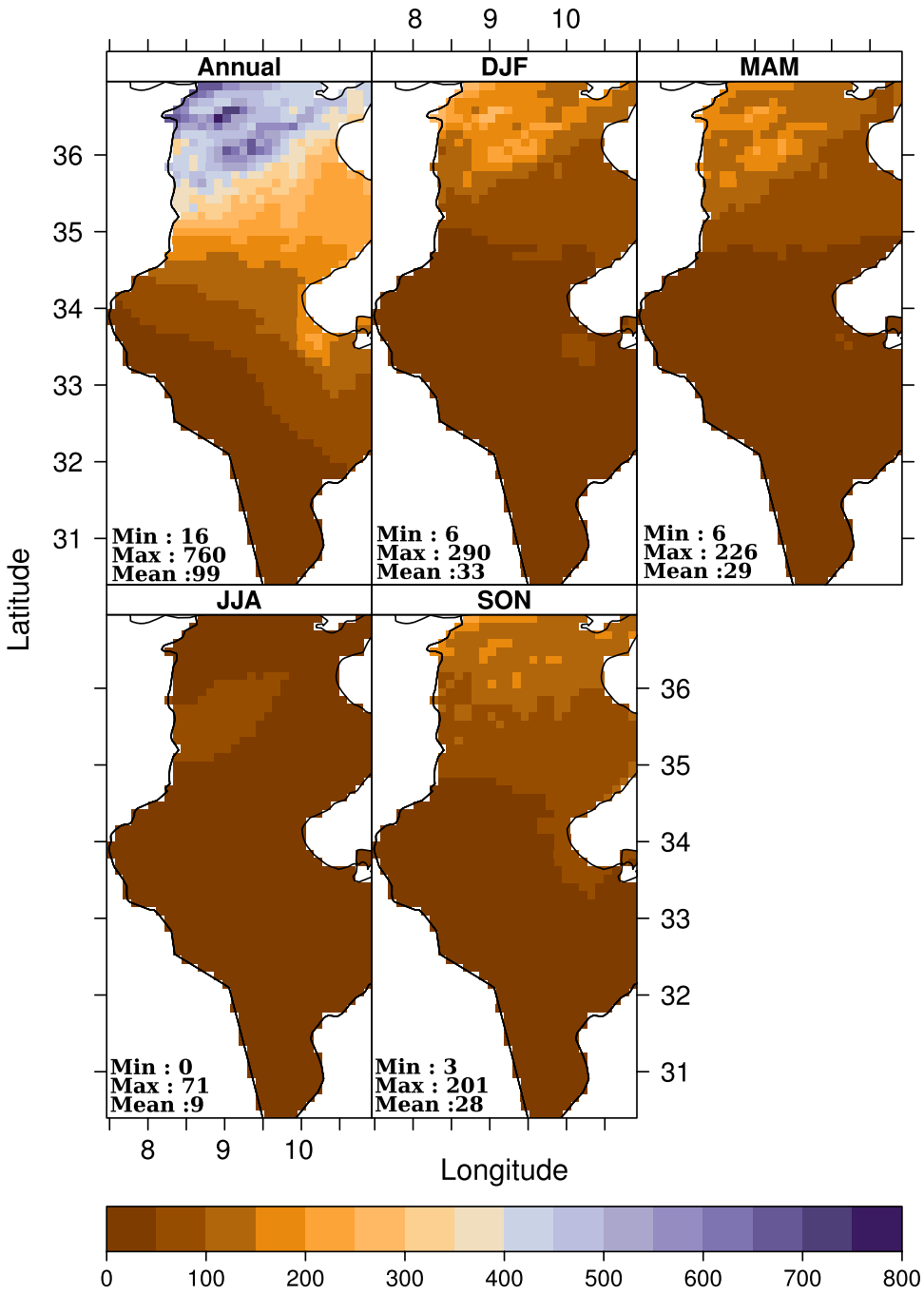

Fig. 4 WRF (ensemble mean)-simulated annual (mm/year) and seasonal (mm/season) rainfall amounts over Tunisia and over the period 1992–2011. The extreme values reached over the domain and the spatial mean are labeled in the figure

in simulating the year-to-year variability of rainfall in Tunisia closely depend on the model and on the season, as evidenced by the temporal correlations of the interannual variability between the spatially averaged annual and seasonal rainfall amounts presented in Table 5. For all simulations, temporal correlation coefficients are higher in DJF than in JJA. Annual correlations are furthermore clearly higher for ERA-I. DHMZ-RegCM shows again bad performance in simulating the rainfall interannual variability as proved by the particularly low and negative temporal correlation coefficients. The interannual bias is exclusively and constantly dry at the annual and DJF timescales for CLMcom-CCLM while it alternates, throughout the study period, between dry and wet for the other simulations.

It is noteworthy again that members of our ensemble are remarkably and steadily convergent in DJF, denoting a strong reproducibility of rainfall interannual variability. In contrast in JJA, members are widely dispersed and drastically deviate from the ensemble mean, hence indicating weak reproducibly and also suggesting that the large-scale control imposed by the lateral boundaries is particularly weakened during this season. We verified this assumption by plotting the temporal

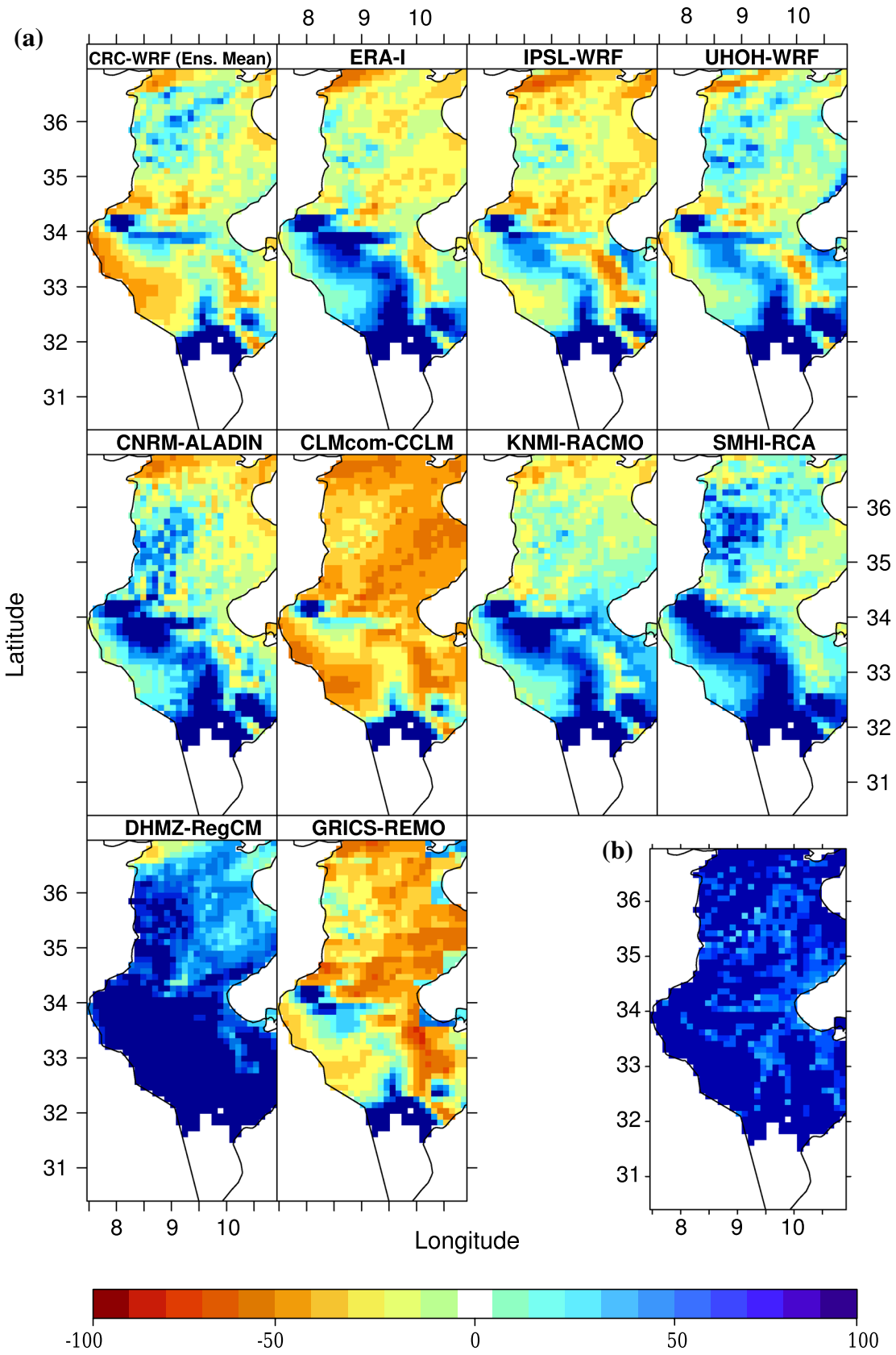

Fig. 5 **a** Annual mean WRF (ensemble mean), ERA-I and a sample of Euro-CORDEX hindcast RCM biases (in percentage) against observation. **b** Percentage of WRF members that are in agreement (i.e. having the same bias sign against observation) with the ensemble mean

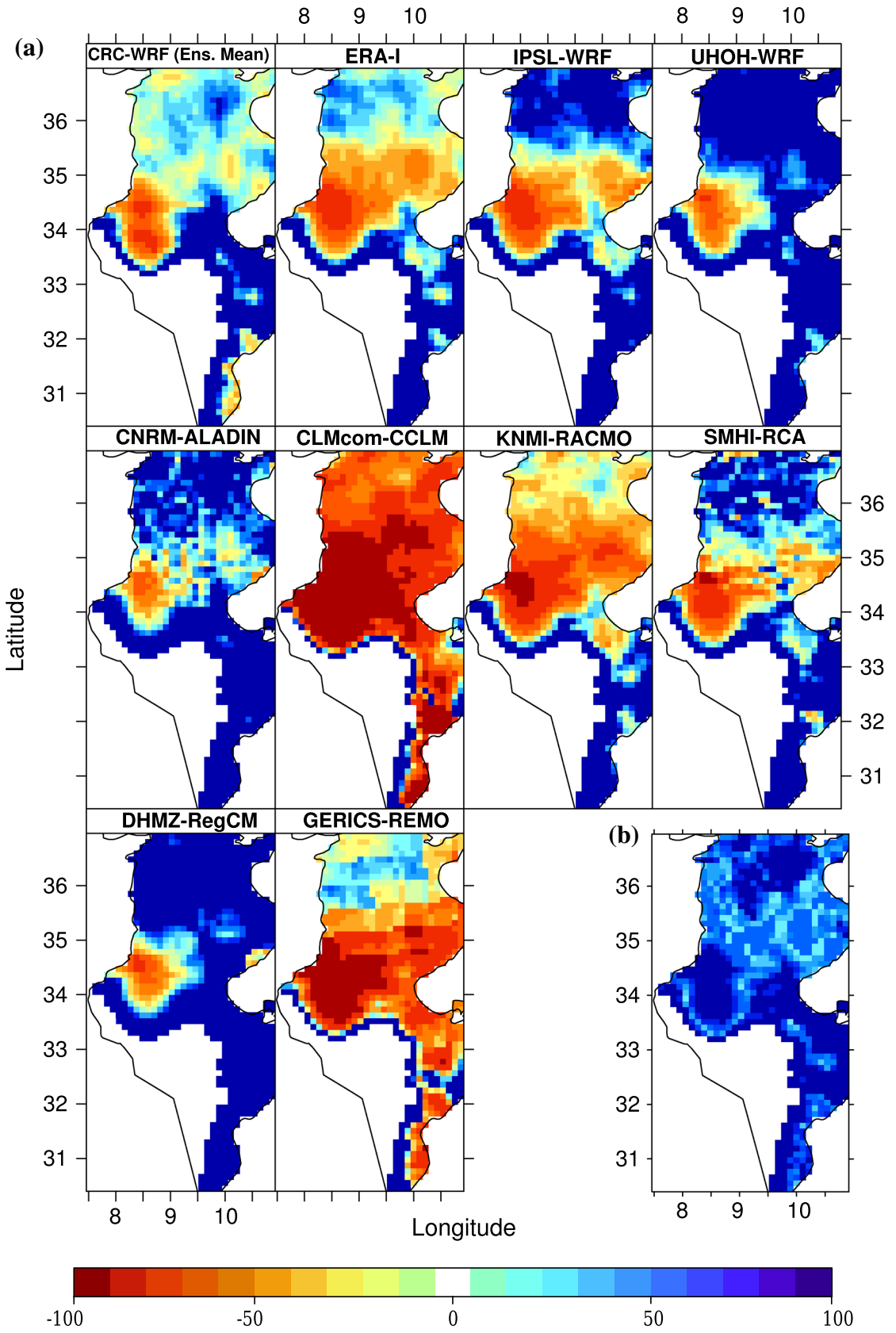

Fig. 6 As Fig. 5 but for JJA seasonal amounts

Table 3 Space–time averaged WRF members (min, max and mean values), ERA-I and the used Euro-CORDEX simulations annual and seasonal simulated rainfall errors and spatial correlations against the Tunisian observational dataset. Computations are made over the period 1992–2008

Simulations	Annual			DJF			JJA		
	MBE (%)	RMSE (%)	R	MBE (%)	RMSE (%)	R	MBE (%)	RMSE (%)	R
WRF members	Min: − 10.46	Min: 34.06	Min: 0.91	Min: 1.59	Min: 43.16	Min: 0.87	Min: 4	Min: 56.96	Min: 0.86
	Max: 9.87	Max: 35.93	Max: 0.92	Max: 11.91	Max: 44.46	Max: 0.88	Max: 59.85	Max: 75.84	Max: 0.89
	Ens. mean: − 1.60	Ens. mean: 33.62	Ens. mean: 0.92	Ens. mean: 5.24	Ens. mean: 43.49	Ens. mean: 0.87	Ens. mean: 29.85	Ens. mean: 60.58	Mean: 0.89
ERA-I	12.44	44.18	0.94	− 16.24	47.72	0.92	15.89	61.34	0.78
IPSL-WRF	− 1.58	38.37	0.92	− 24.01	53.2	0.88	39.86	75.25	0.75
UHOH-WRF	15.55	39.55	0.92	− 16.30	51.57	0.85	74.51	88.61	0.78
CNRM-ALADIN	19.79	46.6	0.88	− 24.64	50.19	0.84	65.4	81.08	0.79
CLMcom-CCLM	− 27.83	44.62	0.96	− 23.44	50.11	0.88	− 64.72	82.64	0.64
KNMI-RACMO	22	43.61	0.97	13.69	47.85	0.82	− 7.16	64.9	0.75
SMHI-RCA	31.66	49.77	0.94	1.22	45.18	0.9	39.23	73.15	0.73
DHMZ-RegCM	72.74	79.23	0.93	44.06	63.86	0.86	79.77	91.36	0.75
GERICS-REMO	− 15.82	42.67	0.87	− 29.15	56.57	0.86	− 29.76	66.94	0.73

interannual correlations between observed (TRMM) and simulated annual and seasonal rainfall amounts in the Mediterranean Basin (Fig. 9). Interannual correlations are computed for each grid point by averaging the interannual correlations of individual members and are statistically significant especially in winter and mostly near the western boundary of the domain, i.e. close to the prevailing westerly large-scale inflow. Nevertheless, both annual and seasonal correlations marginally reach statistical significance east of Greenwich. The constraint of lateral forcing weakens and dissipates by traveling away from the domain's inflow boundary (the concept of "spatial spin-up" as proposed by Leduc and Laprise 2009). The Mediterranean SST forcing is weak regardless of the season since correlations are rarely reaching the significance threshold over the Mediterranean Sea. The spatial spin-up is not constant in time; in particular, it almost vanishes in summer supporting the noisy/stochastic character of the interannual variability of rainfall (at the grid point scale) in summer. Temporal interannual correlations between observed and simulated (WRF_Ens) annual and seasonal rainfall amounts in Tunisia (Fig. 10) are statistically significant north of Tunisia especially in winter (reaching 0.88) when the wettest conditions are recorded in both datasets. Non-significant correlations are obtained south of the domain in JJA and SON.

Table 4 Space–time averaged inter-model and inter-member standard deviations of the annual and seasonal rainfall totals over Tunisia. Computations are made over the period 1992–2008

	Annual	DJF	JJA
Inter-member SD (SD1, mm/day)	0.05	0.03	0.21
Inter-model SD (SD2, mm/day)	0.21	0.22	0.21
Ratio ((SD1/SD2) × 100)	**23.81**	**13.64**	**100**

We further investigated this issue by quantifying, for each grid point of the Tunisian analyzed domain, the fraction of interannual variance that occurs in phase in the ten members and hence interpreted as the reproducible/forced fraction of interannual rainfall variability. The f-ratio (Eq. 7) is presented in Fig. 11, pointing out strong reproducibility of rainfall in winter (domain averaged reproducibility is 90%). The largest fraction of the interannual variability depends consequently on the large-scale forcing. Contrariwise, sensibly lower reproducibility values are found in summer (domain averaged reproducibility is 50%, locally reaching extremely low values south of the domain) and in autumn suggesting therefore that the model is free to generate its own climate in response to small-scale forcings or local processes. The fine-scale convective activity could be one of the main drivers of this stochastic internnual variability significantly revealed in summer and autumn when convective rainfall contributes in fact to ~ 50% of total rainfall in Tunisia as shown in Fig. 12C. Note that the average values of rainfall reproducibility (i.e. f ratio) are smaller than for the parent domain (Appendix). Spatial variability

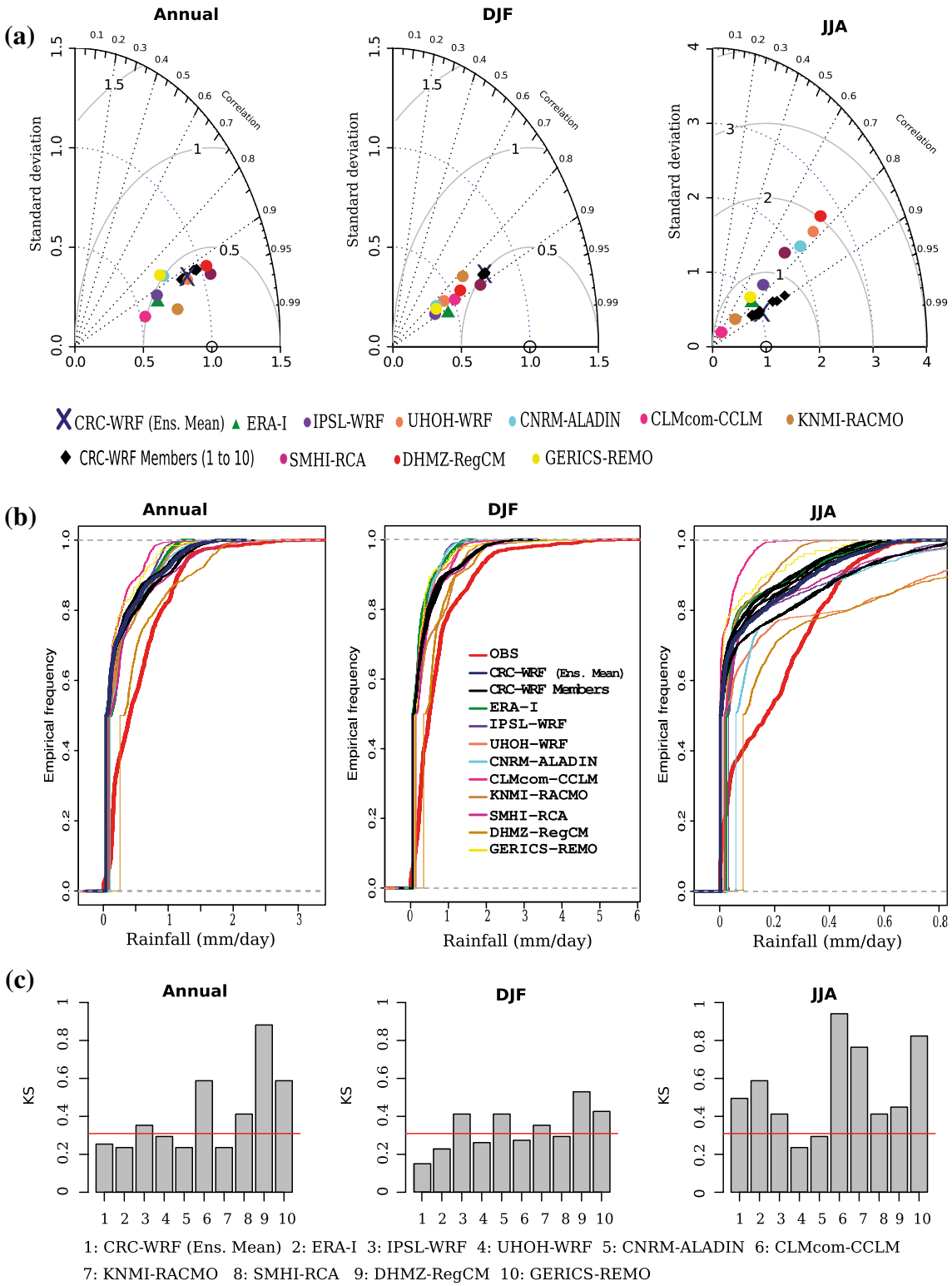

Fig. 7 **a** Spatial annual and seasonal (DJF and JJA) normalized Taylor diagrams exploring and ranking the ERA-I, the WRF ensemble and Euro-CORDEX regional models performance with respect to observation. **b** Spatial empirical Cumulative Distribution Functions of annual and seasonal (DJF and JJA) observed and simulated precipitation over Tunisia. **c** Kolmogorov–Smirnov test statistic between the observed and simulated annual and seasonal space-averaged precipitation CDFs. The horizontal red lines are critical values corresponding to the 5% significance level

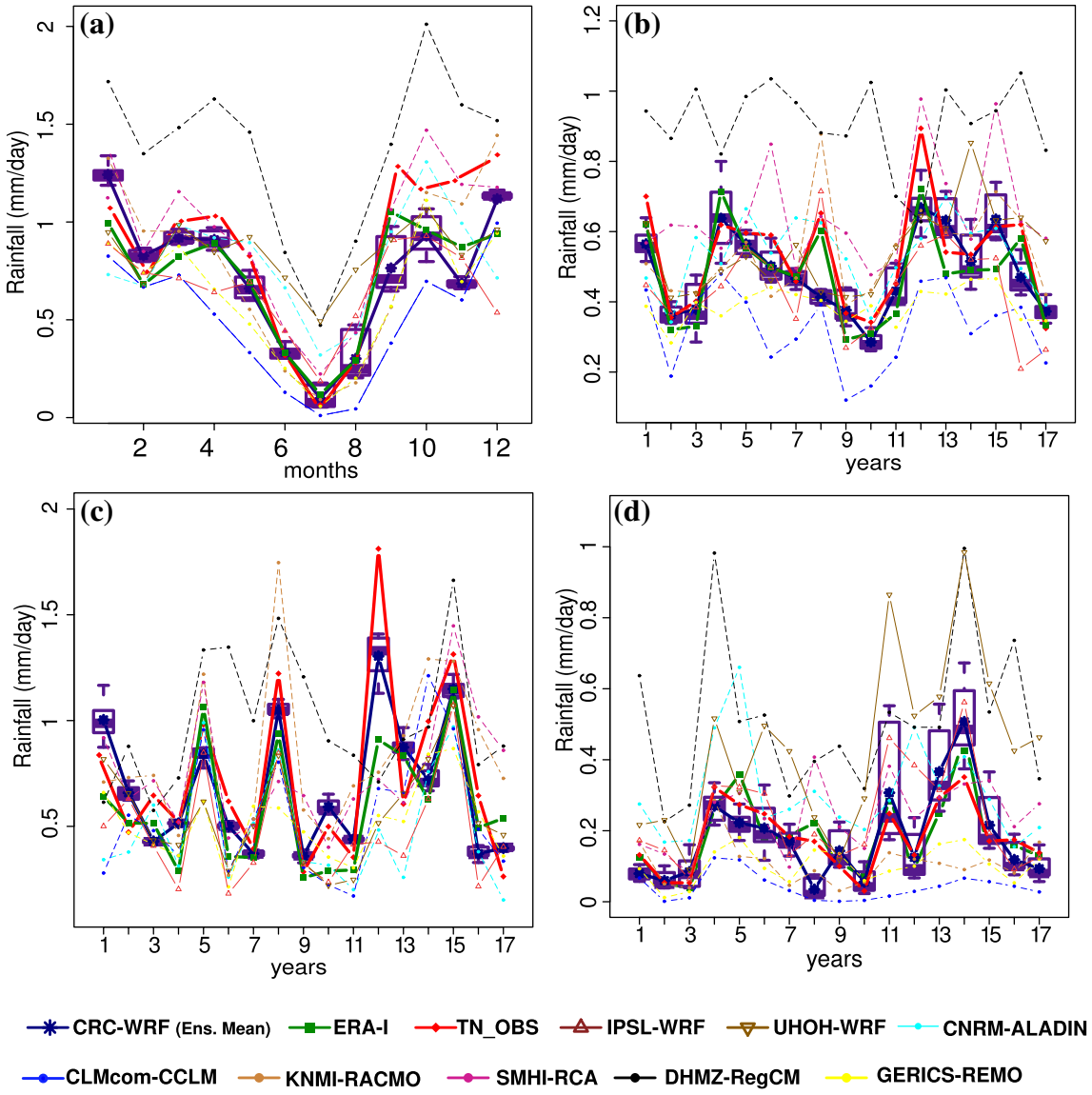

Fig. 8 **a** Mean annual cycle (mm/day) averaged spatially over Tunisia for the observational dataset, ERA-I, the WRF ensemble and the used Euro-CORDEX simulations. Interannual variability of the annual. **b** and seasonal (**c** for DJF and **d** for JJA) rainfall amounts (mm/day) averaged spatially over the Tunisia and for the period 1992–2008

of the inter-member standard deviation (based on Eq. 4) as well as its interannual variability (based on Eq. 5) are moreover presented in Fig. 12. Inter-member standard deviations reaches its maximum (> 7 mm/day) over the Gulf of Gabès (center of Tunisia) and in coastal Tunisia in SON while its temporal evolution (Fig. 12b) shows a non-steady year-to-year fluctuation.

3.2.3 Daily rainfall indexes

Interannual variability of daily precipitation statistics (number of rainy days (P > 1 mm/day), average intensity of rainy days, 99 percentile (p99) of daily rainfall amounts (computed for all days of the study period) for characterizing extreme rainfall and the largest number of consecutive dry days (P < 1 mm/day) is displayed in Fig. 13. Only simulations results are presented since the observed precipitation dataset is provided at a monthly timescale; spatial patterns of daily indexes are not shown because they closely agree with spatial distributions of the precipitation totals. The interannual variability of WRF_Ens rainfall is particularly well explained by the p99 (Fig. 13c) and the mean number of rainy days (Fig. 13a). The average intensity of rainy days (Fig. 13b) shows a quite different temporal pattern since years with heavy or higher number of rainy days do not coincide with years of higher intensity. Intensity of the

Table 5 Temporal correlations of the interannual variability between the spatially averaged annual and seasonal rainfall amounts over Tunisia. Computations and made over the period 1992–2008

	Annual	DJF	JJA
WRF members	Min: 0.76	Min: 0.87	Min: 0.60
	Max: 0.81	Max: 0.88	Max: 0.68
	Ens. mean: 0.79	Ens. mean: 0.88	Ens. mean: 0.63
ERA-I	0.92	0.84	0.7
IPSL-WRF	0.58	0.63	0.56
UHOH-WRF	0.67	0.78	0.6
CNRM-ALADIN	0.45	0.6	0.47
CLMcom-CCLM	0.73	0.75	0.66
KNMI-RACMO	0.63	0.69	0.57
SMHI-RCA	0.6	0.64	0.46
DHMZ-RegCM	− 0.24	0.19	-0.1
GERICS-REMO	0.47	0.58	0.23

summertime rainfall is characterized by high amplitudes and a large member dispersion. With comparison to the other Euro-CORDEX runs, DHMZ-RegCM strongly overestimates the average annual (~ 83) and seasonal (~ 26 in DJF and ~ 10 in JJA) numbers of rainy days, then explaining its overestimation of rainfall amounts (as mentioned in Sect. 3.2.1). Underestimation of rainfall by CLMcom-CCLM can also be explained by a clear underestimation (overestimation) of the average number of rainy days (largest number of consecutive dry days). The highest average seasonal p99 is recorded by KNMI-RACMO (DHMZ-RegCM) in DJF: ~ 7 mm/day (JJA: ~ 3 mm/day).

To characterize the magnitude of interannual spreads between the members of the WRF ensemble and between the used sample of Euro-CORDEX simulations for the daily rainfall indexes, the space-time averaged inter-model and inter-member standard deviations (based on Eq. 6) as well the ratio between these two metrics are computed and then presented in Table 6. Inter-member uncertainties are generally larger in summer than in winter (excepting the 99 percentile of daily rainfall) as proven by values of the inter-member standard deviation and despite the low amounts of the summertime rainfall. Uncertainties are furthermore higher between the Euro-CORDEX models than between the WRF ensemble members. The highest value of the inter-model and inter-member standard deviation ratios concerns the summertime average intensity of rainy days: ~ 85% (this result is also graphically clear in the right-hand panel of Fig. 13b). Standard deviation ratios are computed for the parent domain showing that the inter-model uncertainties are higher than the inter-member spreads at the annual, seasonal and daily time scales.

4 Discussion

The evaluation of the WRF skills in simulating the rainfall spatial and temporal variability over the Mediterranean basin is addressed through comparisons to global observational datasets. The climatological annual cycle of rainfall is marked by its strong seasonality and its unimodal distribution and is well captured by the model in spite of a minor timing error over landmasses. Similar timing errors in WRF are observed by Pohl et al. (2014) over South Africa or by Warrach-Sagi et al. (2013) over Germany. Like Pohl et al. (2014), the simulated timing error seems to be attributed to internal model errors and not to be inherited from the driving ERA-I boundary conditions. The WRF simulation, moreover, remarkably underestimates the summer and early autumn rainfall over landmasses (particularly south of the domain). This fact could be linked to an underestimation of convective rainfall which significantly contributes to total rainfall over the land mainly in summer (~ 63%) and early autumn (~ 50%).

The evaluation of the WRF ensemble and a sample of Euro-CORDEX RCMs skills in simulating the rainfall spatial and temporal variability over Tunisia is addressed through comparisons to a local rain gauges dataset. Space-time averaged biases over Tunisia are wet in both DJF and JJA seasons and considerably vary in JJA for the WRF ensemble while there are season-dependent (dry in DJF and wet in JJA) for most of the Euro-CORDEX simulations. These findings differ from Kotlarski et al. (2014) who studied the European climate from Euro-CORDEX RCM ensembles at 12 and 50 km grid resolutions. The authors reported indeed a wet bias against E-OBS dataset for both DJF and JJA seasons and over most parts of Europe being more pronounced in the 12 km simulations. Katragkou et al. (2015) investigated also six Euro-CORDEX WRF simulations with different physical configurations and described wet bias for both seasons and over all the European subregions. Summer precipitation wet biases are stronger in simulations with the Kain–Fritsch convective parameterization according to the same authors. The lack of cumulus cloud feedbacks to radiation in early versions of the WRF model (e.g., 3.3) results, moreover, in precipitation biases according to Alapaty et al. (2012). Such an issue is rectified in recent versions of WRF. Unlike our results, Bargaoui et al. (2013) who used 6 ENSEMBLES RCM model runs at 25 km spatial resolution over the period 1961–2000 and restricted their analyses to the north of Tunisia, report that all models tend to underestimate total precipitation except some grid cells close to the Algerian borders. No clear orographic effect is moreover found at the 25 km

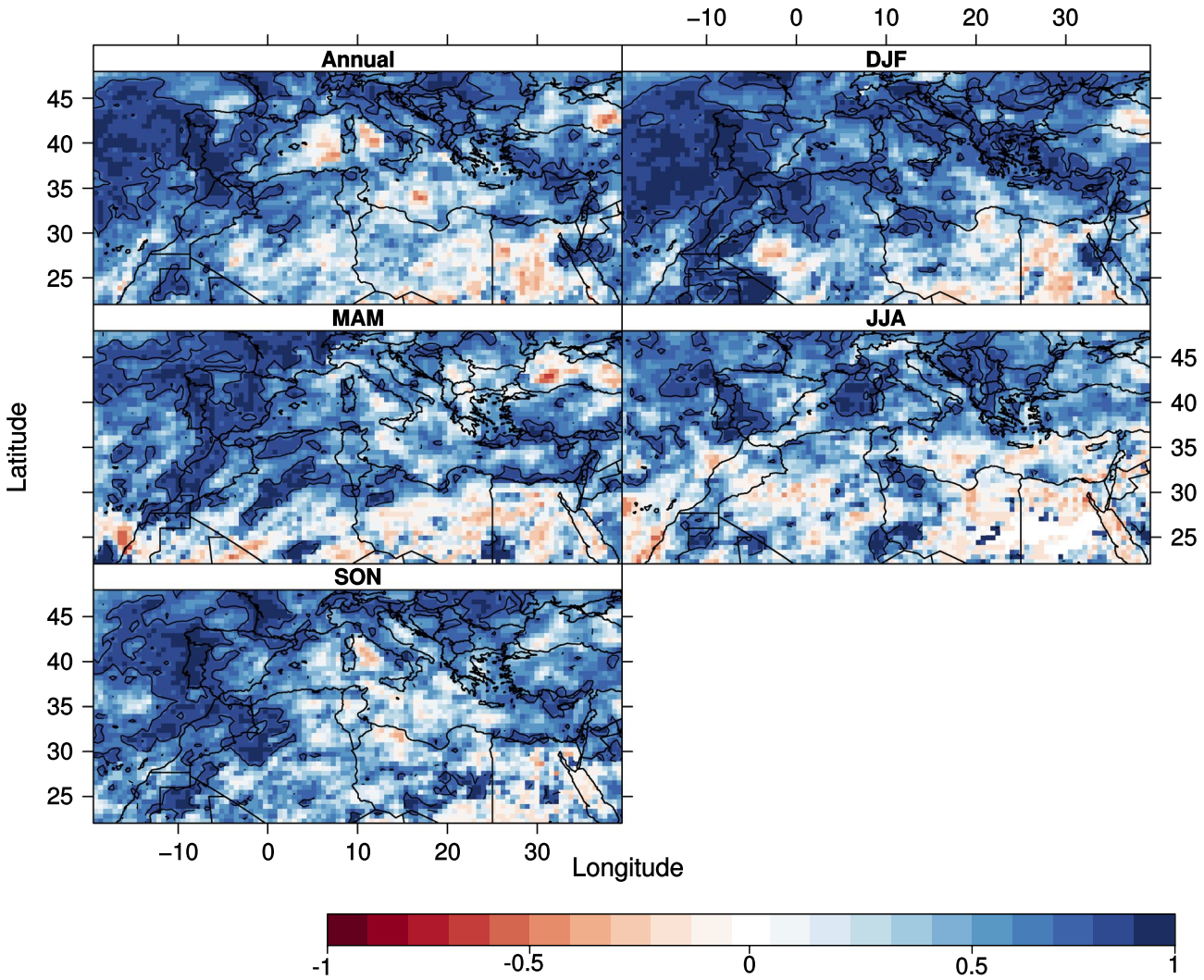

Fig. 9 Interannual correlations of rainfall amounts for each grid-point of the Mediterranean analyzed domain between the WRF simulations (see text for details) and TRMM, calculated for annual rainfall and each season. 95% significant correlations according to a Bravais-Pearson test are shown by solid black curves

spatial resolution. Some of the revealed biases in this work seem, nonetheless, not to be linked to models deficiencies, but could be rather related to imperfections in the rainfall data interpolation process. The mean annual and DJF wet biases in the west center (the salt land depressions) and the far south of Tunisia found in all simulations could be indeed due to the extreme scarcity of rain gauges and consequently to the spatial smoothing.

Models skills are also season-dependent. In agreement with Kotlarski et al. (2014), temporal correlation between the simulated and observed mean annual and seasonal rainfall totals over Tunisia are systematically higher in DJF than in JJA. This could be explained by the fact that models are more constrained by the temporal evolution of ERA-I lateral forcing in DJF since the wintertime Mediterranean climate is more affected by large-scale features (e.g., Kotlarski et al. 2014). However, the DJF temporal correlations we obtained remain lower than those obtained by Kotlarski et al. (2014) over Europe. Although we do not have a definite explanation, this finding may reflect a geographic dependency of the models performance. Overall, temporal correlations are higher for the WRF ensemble than for the Euro-CORDEX simulations. This could be explained by the central location of Tunisia within the regional domain (i.e. far from the ERA-I boundary forcing unlike its position within the Euro-CORDEX domain) allowing an appropriate representation of local circulation patterns. The WRF ensemble also shows good performance in downscaling the summertime precipitation spatial variability over Tunisia. The model, with the highest spatial correlation coefficient, is indeed best capturing the spatial variability of precipitation. Similar results are obtained in the same experiment for spatial variability

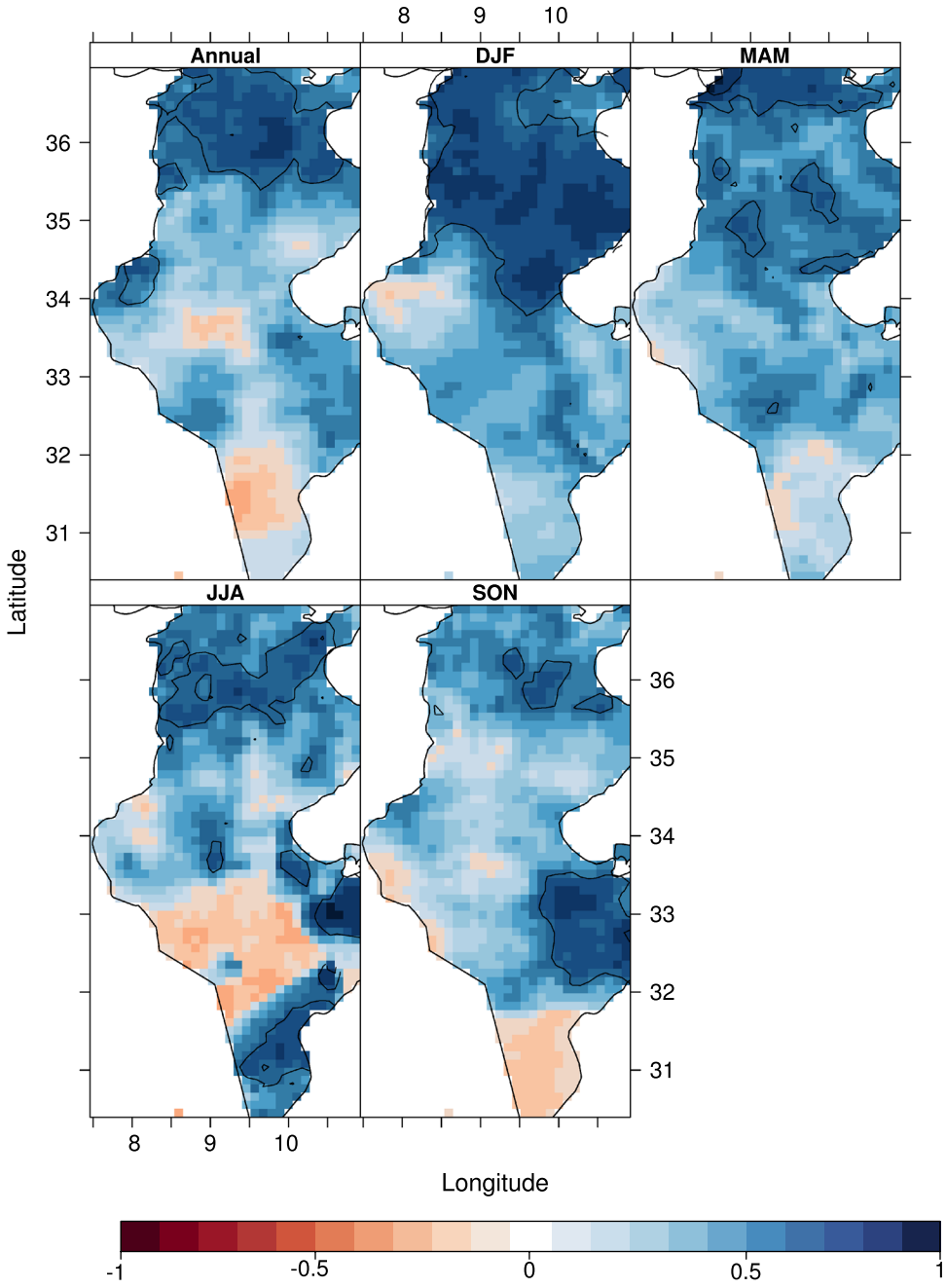

Fig. 10 As Fig. 9 but for the correlations computed between the WRF simulations (Tunisia) and observations

of the Tunisian near surface air temperatures in JJA (Fathalli et al. 2016).

The sources of inter-model spreads within the Euro-CORDEX framework are well discussed in Vautard et al. (2013) and Kotlarski et al. (2014) and specifically Katragkou et al. (2015). These studies mainly incriminate the use of different physical parameterizations (especially the choice of the convective scheme) and the way land surface-atmosphere fluxes are resolved by the models. Katragkou et al. (2015) also pointed out the lack of a specific configuration that seem to totally mitigate the WRF wet biases over Europe. Inter-member spreads of the annual and seasonal rainfall totals and some studied daily indexes (excepting for the 99 percentile of daily rainfall) are stronger in JJA than in DJF. This could be explained by the importance of regional and local scale summertime processes. The large convective contribution combined with a drastically reduced constraint of the lateral forcing on the regional climate (anticyclones are more persistent during summer and the low-pressure systems are 70% less frequent than in winter over Europe and the Mediterranean regions according to Elizalde 2011), could in fact promote a strong inter-member spread given the non-linear nature of the sub-grid scale (i.e. locally resolved) convection process

(Sieck et al. 2013). Inter-member spreads are, furthermore, equal to the inter-model uncertainties when simulating the JJA rainfall totals over Tunisia. Internal variability does not significantly change the WRF domain-wide solutions (mean rainfall climatology) over the Mediterranean Basin (Table 2) contrary to what it does over the nested domain. Our results (Table 3) show indeed that the sign of the WRF mean annual rainfall biases over Tunisia can unexpectedly change from one member to another. Moreover, space-time averaged WRF biases substantially vary from one member to another in summer.

These results should be particularly considered with precaution since they are obtained with a specific configuration of the WRF model, and then should be tested for other physical parameterization schemes, other variables (e.g. temperature), other small domains and other RCMs. Crétat and Pohl (2012) showed indeed that internal variability of rainfall over southern Africa simulated with WRF is physic-dependent at different time scales. Laprise et al. (2012) using the CRCM model in a 20-member ensemble simulation over North America noted that the simulated internal variability is much stronger for precipitation than for temperature.

Fig. 12 **a** Inter-member standard deviation between the annual and seasonal rainfall daily amounts (mm/day) simulated by the individual WRF members and over the Tunisian analyzed domain. **b** Interannual variability of the WRF-simulated rainfall standard deviation. **c** Average annual cycle of convective rainfall contributions to total amounts (%) ▶

5 Conclusion

We provided in this paper a first attempt to evaluate rainfall over Tunisia (at ~12 km spatial resolution) analyzed in a ten-member ensemble simulation performed using the WRF model, and in a multi-RCM hindcast within the Euro-CORDEX initiative. Analyses of the simulations are carried out at the annual, seasonal and daily timescales and are compared

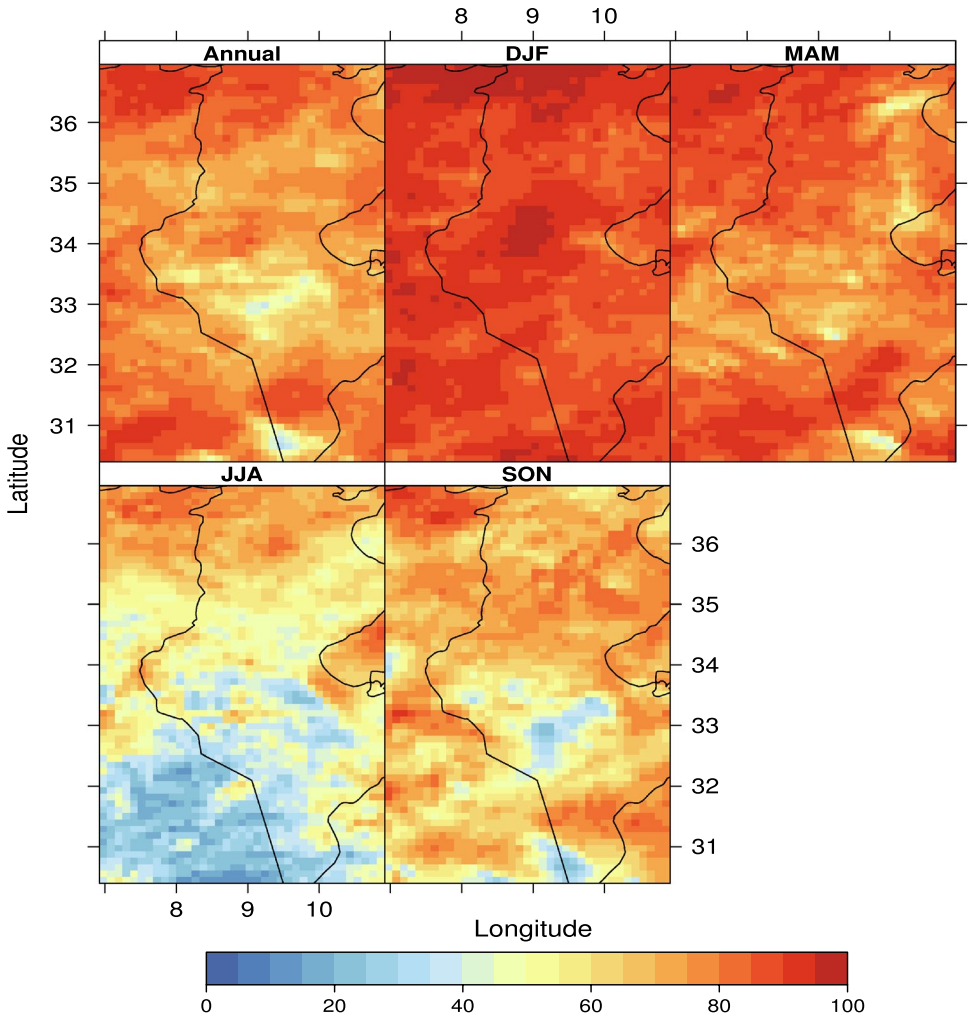

Fig. 11 Reproducible fraction (%) of interannual rainfall variability for each grid point of the Tunisian analyzed domain (see text for definition), calculated for annual rainfall and each season. See text for computation and presentation details

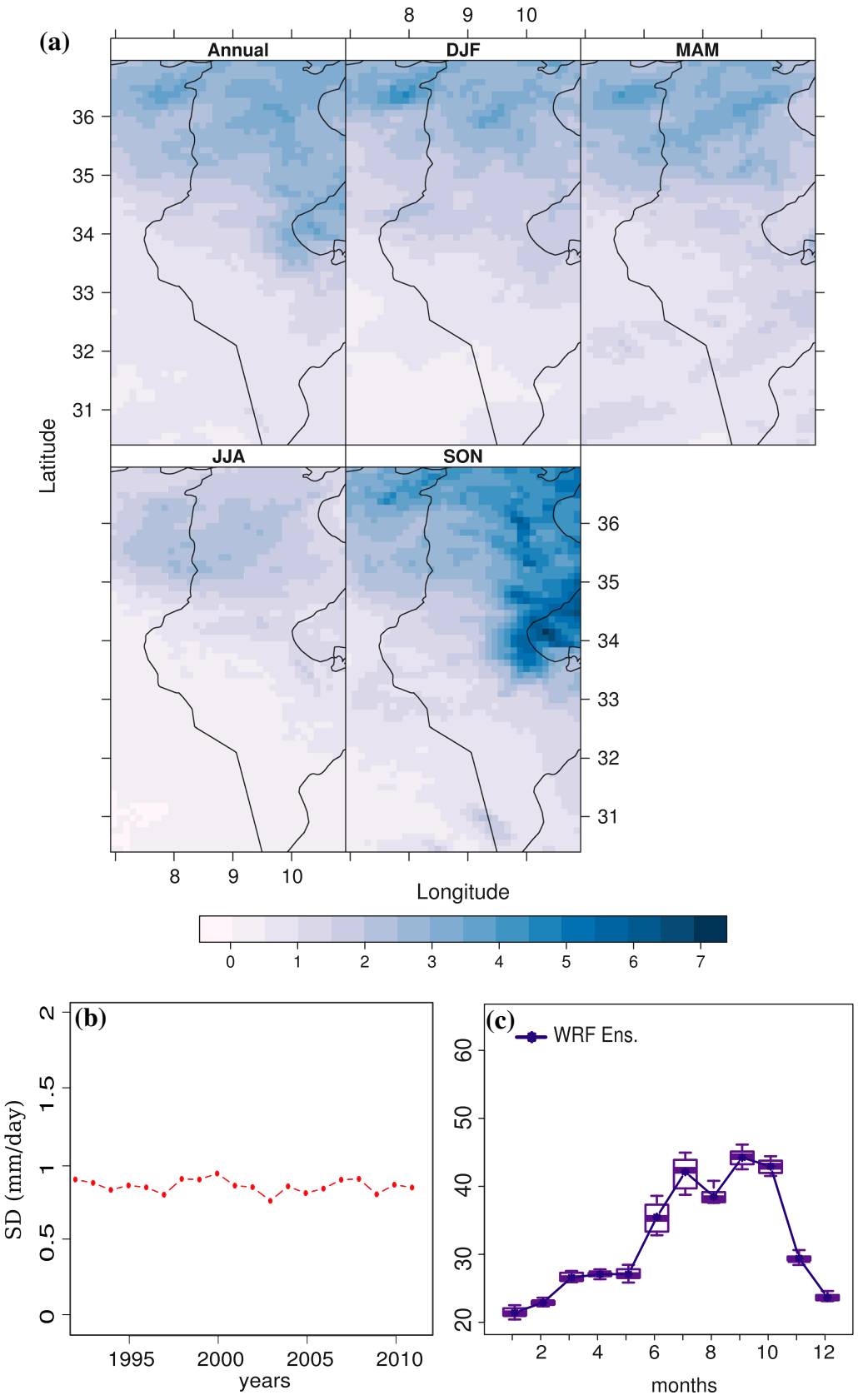
(a)
Annual
DJF
MAM
JJA
SON
Latitude
Longitude
8
9
10
31
32
33
34
35
36
0
1
2
3
4
5
6
7
(b)
SD (mm/day)
years
1995
2000
2005
2010
(c)
WRF Ens.
months
2
4
6
8
10
12
20
30
40
50
60

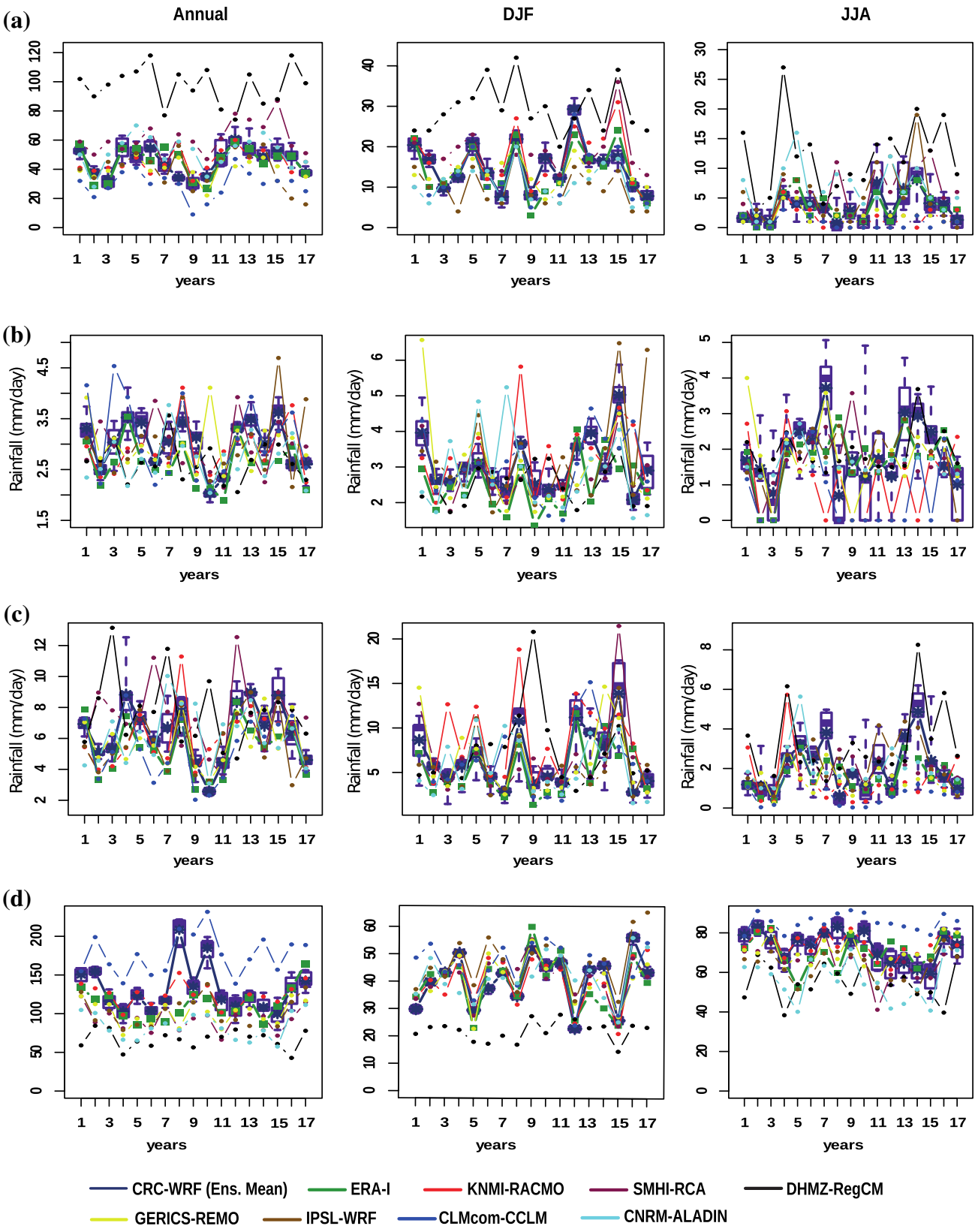

Fig. 13 **a** Interannual variability of the simulated number of rainy days ($P \geq 1$ mm/day) according to the WRF ensemble, ERA-I and a sample of Euro-CORDEX simulations, calculated each year and each DJF and JJA season and averaged spatially over Tunisia. **b** As **a** but for average intensity of rainy days (mm/day). **c** As **a** but for the 99th percentile value (p99 in mm/day) of daily rainfall amounts. **d** As **a** but for the largest number of consecutive dry days ($P < 1$ mm/day)

Table 6 As Table 4 but for the rainfall daily indexes

	Annual	DJF	JJA
Number of rainy days			
Inter-member SD (SD1)	4.48	1.33	1.69
Inter-model SD (SD2)	23.17	7.36	4.57
Ratio [(SD1/SD2)×100]	**19.33**	**18.07**	**36.98**
Intensity of rainy days			
Inter-member SD (SD1, mm/day)	0.18	0.26	0.66
Inter-model SD (SD2, mm/day)	0.54	0.82	0.78
Ratio [(SD1/SD2)×100]	**31.58**	**31.70**	**84.62**
99 percentile of daily rainfall			
Inter-member SD (SD1, mm/day)	0.7	0.93	0.79
Inter-model SD (SD2, mm/day)	2.05	3.14	1.13
Ratio [(SD1/SD2)×100]	**28**	**29.62**	**69.91**
Largest number of consecutive dry days			
Inter-member SD (SD1)	10.22	0.96	4.41
Inter-model SD (SD2)	37	9.37	11.96
Ratio [(SD1/SD2)×100]	**27.62**	**10.25**	**36.87**

to a dense network of local rain gauges. This experimental protocol allows quantifying, on the one hand, the errors associated with the simulations, and on the other hand, the forced (i.e. reproducible) and stochastic (i.e. unreproducible) components of regional climate variability. Indeed, the WRF 10-member ensemble allows us to address the uncertainties due to model's internal variability when the initial conditions are the only parameter that differ between the simulations, and then brings an added information concerning the respective magnitude of the inter-member spreads and inter-model uncertainties. These are due to the use of different RCM dynamic and physical configurations. Uncertainties are here addressed using a simple spread metric (standard deviation). Precipitation in the Mediterranean Basin at 60 km grid spacing is also considered by comparing the WRF simulation to the driving ERA-I reanalysis and to various gridded rainfall datasets mainly showing that WRF (ensemble mean) overestimates mean annual rainfall amounts mostly along the main European mountain ranges and over the eastern Mediterranean Sea. It underestimates rainfall south of the domain. The model is furthermore unable to improve upon its driver (i.e. ERA-I main spatial biases being reproduced more intensely by WRF).

Over Tunisia, WRF (the ten-member ensemble mean) shows overall good capabilities in simulating spatial patterns of mean annual and seasonal rainfall amounts (mainly the altitudinal and latitudinal gradients), as well as the rainfall temporal variability (seasonality and interannual fluctuations) in spite of some systematic errors. Skills in simulating rainfall variability by the sample of Euro-CORDEX RCM simulations globally depend on the model and the season excepting a systematic overestimation (underestimation) of rainfall amounts by RegCM (CCLM). Ratios between the inter-member and inter-model standard deviation show that the inter-model spreads are globally higher at the annual, seasonal and daily time scales. Inter-member uncertainties can nonetheless be of the same magnitude. This result particularly concerns the simulated JJA rainfall totals over Tunisia. The stochastic component of a regional climate signal mainly expressed in summer then should be taken into account when ranking multi-model regional simulations.

The reproducibility of the interannual variability of rainfall is furthermore estimated, at the grid point scale, through the *f* ratio which allows us indeed to quantify the forced vs. stochastic fractions of rainfall variability, together with its seasonal dependency. Strong reproducibility values are particularly obtained in winter, likely indicative of a stronger large-scale control. In summer, rainfall is by cons much less reproducible. Model members are widely dispersed around the ensemble mean, thus suggesting that the Tunisian summertime rainfall is more related to small-scale (local to regional) and possibly non-linear processes, regional models are then more free to develop their own climate and consequently to generate larger uncertainties. At this stage, a further understanding of the model errors is required, including the recurrent seasonal phasing of some biases and the growth of uncertainties in summer when convective processes predominate. These issues will be addressed in a future work focused on shorter timescales and adopting a weather regime approach to decompose the simulated anomalies, errors and internal variability in terms of recurrent synoptic configurations.

Acknowledgements We thank two anonymous reviewers for their comments that remarkably helped improve this study. WRF was provided by the University Corporation for Atmospheric Research website (for more information see http://www.mmm.ucar.edu/wrf/users/download/). ERA-Interim data were provided by the ECMWF. Calculations were performed using HPC resources from PSIUN-CCUB, Université de Bourgogne Franche-Comté (France). Euro-CORDEX data is downloaded from the "Earth System Grid Federation: ESGF" nodes (http://www.euro-cordex.net/060378/index.php.en). We acknowledge Dr. Kirsten Warrach-Sagi from the University of Hohenheim (Germany) for providing the UHOH WRF simulation data. We also acknowledge Lotfi Boughrara from the "DGRE" of Tunisia and the CRU, UDEL, TRMM, GPCC and GPCP datasets providers for providing precipitation records.

Appendix

See Fig. 14.

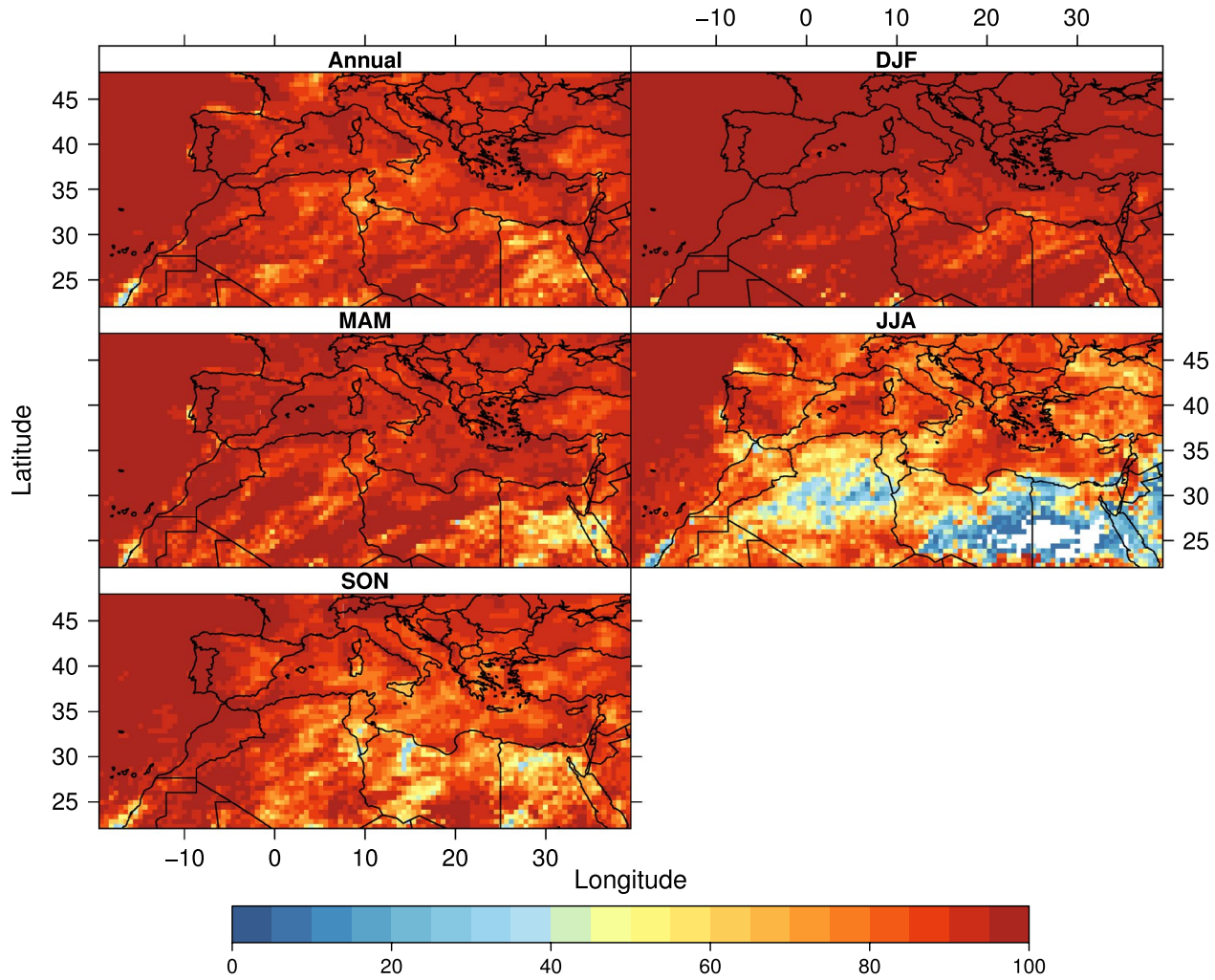

Fig. 14 As Fig. 11 but for the Mediterranean domain

References

Adler RF, Huffman GJ, Chang A, Ferraro R, Xie P, Janowiak J, Rudolf B, Schneider U, Curtis S, Bolvin D, Gruber A, Susskind J, Arkin P (2003) The version 2 Global Precipitation Climatology Project (GPCP) precipitation analysis (1979-present). J Hydrometeorol 4:147–1167

Alapaty K, Herwehe JA, Otte TL, Nolte CG, Bullock OR, Mallard MS, Kain JS, Dudhia J (2012) Introducing subgrid-scale cloud feedbacks to radiation for regional meteorological and climate modeling. Geophys Res Lett 39:L24808. https://doi.org/10.1029/2012GL054031 2012.

Alexandru A, de Elia R, Laprise R (2007) Internal variability in regional climate downscaling at the seasonal scale. Mon Weather Rev 135:3221–3238. https://doi.org/10.1175/MWR3456.1

Alvarez O, Guo Q, Klinger RC, Li W, Doherty P (2014) Comparison of elevation and remote sensing derived products as auxiliary data for climate surface interpolation. Int J Climatol 34:2258–2268. https://doi.org/10.1002/joc.3835

Bargaoui Z, Tramblay Y, Lawin EA, Servat E (2013) Seasonal precipitation variability in regional climate simulations over Northern basins of Tunisia. Int J Climatol. https://doi.org/10.1002/joc.3683

Bénard P, Vivoda J, Masek J, Smolikova P, Yessad K, Smith C, Brozkova R, Geleyn GF (2010) Dynamical kernel of the Aladin-NH spectral limited-area model: formulation and sensitivity experiments. Q J R Meteor Soc 136:155–169

Berndtsson R (1987) Spatial and temporal variability of rainfall and potential evaporation in Tunisia. Proceedings of the Vancouver Symposium, IAHS Publ, p 168

Berndtsson R (1989) Topographical and coastal influence on spatial precipitation patterns in Tunisia. Int J Climatol 9:357–369

Bosilovich M, Chen J, Robertson FR, Adler RF (2008) Evaluation of global precipitation in reanalyses. J Appl Meteorol Climatol 47:2279–2299. https://doi.org/10.1175/2008JAMC1921.1

Brands S, Herrera S, Fernandez J, Gutiérrez JM (2013) How well do CMIP5 Earth System Models simulate present climate conditions in Europe and Africa? Clim Dyn 41:803–817. https://doi.org/10.1007/s00382-013-1742-8

Brown JC, Gupta A, Brown JR, Muir L, Risbey JS, Whetton P, Zhang X, Ganachaud A, Murphy B, Wijffels SE (2013) Implications of CMIP3 model biases and uncertainties for climate projections in the western tropical Pacific. Clim Change 119:147–161. https://doi.org/10.1007/s10584-012-0603-5

Camera C, Bruggeman A, Hadjinicolaou P, Michaelides S, Lange MA (2014) Evaluation of interpolation techniques for the creation of

gridded daily precipitation (1 × 1 km2); Cyprus, 1980–2010. J Geophys Res Atmos 119:693–712. https://doi.org/10.1002/2013JD020611

Cavicchia L, Scoccimarro E, Gualdi S, Marson P, Ahrens B, Berthou S et al (2016) Mediterranean extreme precipitation: a multi-model assessment. Clim Dyn. https://doi.org/10.1007/s00382-016-3245-x

Caya D, Biner S (2004) Internal variability of RCM simulations over an annual cycle. Clim Dyn 22:33–46. https://doi.org/10.1007/s00382-003-0360-2

Ceccato P, Dinku T (2010) Introduction to remote sensing for monitoring rainfall, temperature, vegetation and water bodies. International Research Institute for Climate and Society Earth Institute, Columbia University, Technical Report 10–04, p 15. https://iri.columbia.edu/~pceccato/Remote_Sensing_Introduction/Introduction_to_remote-sensing-environmental_monitoring.pdf

Chen F, Dudhia J (2001) Coupling an advanced land surface—hydrology model with the Penn State—NCAR MM5 modeling system. Part I: Model implementation and sensitivity. Mon Weather Rev 129:569–585. https://doi.org/10.1175/1520-0493(2001)129<0569:CAALSH>2.0.CO;2

Christensen OB, Gaertner MA, Prego JA, Polcher J (2001) Internal variability of regional climate models. Clim Dyn 17:875–887

Crétat J, Pohl B (2012) How physical parameterizations can modulate internal variability in a regional climate model. J Atmos Sci 69:714–724. https://doi.org/10.1175/JAS-D-11-0109.1

Crétat J, Macron C, Pohl B, Richard Y (2011a) Quantifying internal variability in a regional climate model: a case study for Southern Africa. Clim Dyn 37:1335–1356. https://doi.org/10.1007/s00382-011-1021-5

Crétat J, Pohl B, Richard Y, Drobinski P (2011b) Uncertainties in simulating regional climate of Southern Africa: sensitivity to physical parameterizations using. WRF. Clim Dyn 38:613–634

Dai A, Wigley TML (2000) Global patterns of ENSO-induced precipitation. Geophys Res Lett 27:1283–1286

Darling DA (1957) The Kolmogorov-Smirnov, Cramer-von Mises Tests. Ann Math Stat 28(4):823–838. https://doi.org/10.1214/aoms/1177706788

Dee DP, Uppala SM, Simmons AJ et al (2011) The ERA-Interim reanalysis: configuration and performance of the data assimilation system. Q J R Meteorol Soc 137:553–597. https://doi.org/10.1002/qj.828

Diaconescu EP, Laprise R, Sushama L (2007) The impact of lateral boundary data errors on the simulated climate of a nested regional climate model. Clim Dyn 28:333–350

Drobinski P, Anav A, Lebeaupin-Brossier C et al (2012) Model of the regional coupled earth system MORCE: application to process and climate studies in vulnerable regions. Environ Model Softw 35:1–18. https://doi.org/10.1016/j.envsoft.2012.01.017

Dudhia J (1989) Numerical study of convection observed during the winter monsoon experiment using a mesoscale two-dimensional model. J Atmos Sci 46:3077–3107

Duffy PB, Arritt RW, Coquard J, Gutowski W, Han J, Iorio J, Kim J, Leung LR, Roads J, Zeledon E (2006) Simulations of present and future climates in the western U.S. with four nested regional climate models. J Clim 19:873–895

Elizalde A (2011) The water cycle in the Mediterranean region and the impacts of climate change, vol 103. Max Planck Institute for Meteorology Rep on Earth System Science, p 128. https://www.mpimet.mpg.de/fileadmin/publikationen/Reports/WEB_BzE_103.pdf

Fathalli B, Pohl B, Castel T, Safi MJ (2016) Dynamical downscaling of temperature variability over Tunisia: evaluation a 21-year-long simulation performed with the WRF model. J Climatol Weather Forecast 4:166. https://doi.org/10.4172/2332-2594.1000166

Feki H, Slimani M, Cudennec C (2012) Incorporating elevation in rainfall interpolation in Tunisia using geostatistical methods. Hydrol Sci J 57:1294–1314. https://doi.org/10.1080/02626667.2012.710334

Fernandez J, Montavez JP, Sanez J, Gonzalez-Rouco JF, Zorita E (2007) Sensitivity of the MM5 mesoscale model to physical parameterizations for regional climate studies: annual cycle. J Geophys Res 112:D04101. https://doi.org/10.1029/2005JD006649

Flaounas E, Bastin S, Janicot S (2010) Regional climate modelling of the 2006 West African monsoon: sensitivity to convection and planetary boundary layer parameterisation using WRF. Clim Dyn 36:1083–1105

Flaounas E, Drobinski P, Vrac M, Bastin S, Lebeaupin-Brossier C, Stéfanon M, Borga M, Calvet JC (2013) Precipitation and temperature space-time variability and extremes in the Mediterranean region: evaluation of dynamical and statistical downscaling methods. Clim Dyn 40:2687–2705. https://doi.org/10.1007/s00382-012-1558-y

Friedl MA, McIver DK, Hodges JCF, Zhang XY, Muchoney D, Strahler AH, Woodcock CE, Gopal S, Schneider A, Cooper A, Baccini A, Gao F, Schaaf C (2002) Global land cover mapping from MODIS: algorithms and early results. Remote Sens Environ 83:287–302

Giorgi F, Bi X (2000) A study of internal variability of a regional climate model. J Geophys Res 105(D24):29503–29521. https://doi.org/10.1029/2000JD900269

Giorgi F, Cappola E, Solmon F et al (2012) RegCM4: model description and preliminary tests over multiple CORDEX domains. Clim Res 52:7–29

Gómez-Navarro JJ, Montávez JP, Wagner S, Zorita E (2013) A regional climate palaeosimulation for Europe in the period 1500–1990—part 1: model validation. Clim Past 9:1667–1682. https://doi.org/10.5194/cp-9-1667-2013

Gómez-Navarro JJ, Bothe O, Wagner S, Zorita E, Werner JP, Luterbacher J, Raible CC, Montávez JP (2015) A regional climate palaeosimulation for Europe in the period 1500–1990—part 2: shortcomings and strengths of models and reconstructions. Clim Past 11:1077–1095

Harris I, Jones PD, Osborn TJ, Lister DH (2014) Updated high-resolution grids of monthly climatic observations—the CRU TS3.10 Dataset. Int J Climatol 34:623–642. https://doi.org/10.1002/joc.3711

Haylock MR, Hofstra N, Klein Tank AMG, Klok EJ, Jones PD, New M (2008) A European daily high resolution gridded data set of surface temperature and precipitation for 1950–2006. J Geophys Res 113:D20119. https://doi.org/10.1029/2008JD010201

Hertig E, Paxian A, Vogt G, Seubert S, Paeth H, Jacobeit J (2012) Statistical and dynamical downscaling assessments of precipitation extremes in the Mediterranean area. Meteorol Z 21:61–77. https://doi.org/10.1127/0941-2948/2012/0271

Hewitt CD (2004) Ensembles-based predictions of climate changes and their impacts. Eos Trans AGU 85(52):566–566. https://doi.org/10.1029/2004EO520005

Hijmans RJ, Cameron SE, Parra JL, Jones PG, Jarvis A (2005) Very high resolution interpolated climate surfaces for global land areas. Int J Climatol 25:1965–1978. https://doi.org/10.1002/joc.1276

Holtanova E, Kalvova J, Pisoft P, Miksovsky J (2014) Uncertainty in regional climate model outputs over the Czech Republic: the role of nested and driving models. Int J Climatol 34:27–35 (2014). https://doi.org/10.1002/joc.3663

Hong SY, Lim JOJ (2006) The WRF single-moment 6-class microphysics scheme (WSM6). J Kor Meteorol Soc 42:129–151

Hong Y, Nix HA, Hutchinson MF, Booth TH (2005) Spatial interpolation of monthly mean climate data for China. Int J Climatol 25:1369–1379. https://doi.org/10.1002/joc.1187

Hong SY, Noh Y, Dudhia J (2006) A new vertical diffusion package with an explicit treatment of entrainment processes. Mon Weather Rev 134:2318–2341

Huffman GJ, Bovlin DT (2017) Real-Time TRMM Multi-Satellite Precipitation Analysis Data Set Documentation. ftp://trmmopen.gsfc.nasa.gov/pub/merged/V7Documents/3B4XRT_doc_V7.pdf

Huffman GJ, Adler RF, Arkin PA, Chang A, Ferraro R, Gruber A, Janowiak J, Joyce RJ, McNab A, Rudolf B, Schneider U, Xie P (1997) The Global Precipitation Climatology Project (GPCP) combined precipitation data set. Bull Am Meteor Soc 78:5–20

Jacob D, Petersen J, Eggert B et al (2007) EURO-CORDEX: new high-resolution climate change projections for European impact research. Reg Environ Change 14:563. https://doi.org/10.1007/s10113-013-0499-2

Jacob D, Elizalde A, Haensler A, Hagemann S, Kumar P, Podzun R, Rechid D, Remedio AR, Saeed F, Sieck K, Teichmann C, Wilhelm C (2012) Assessing the transferability of the regional climate model REMO to different coordinated regional climate downscaling experiment (CORDEX) regions. Atmosphere 3:181–199. https://doi.org/10.3390/atmos3010181

Jarvis A, Reuter HI, Nelson A, Guevara E (2008) Hole-filled SRTM for the globe Version 4, available from the CGIAR-CSI SRTM 90 m Database. http://www.cgiar-csi.org/data/srtm-90m-digital-elevation-database-v4-1

Kain JS (2004) The Kain–Fritsch convective parameterization: an update. J Appl Meteorol 43:170–181

Katragkou E, Garcia-Diez M, Vautard R et al (2015) Regional climate hindcast simulations within EURO-CORDEX: evaluation of a WRF multi-physics ensemble. Geosci Model Dev 8:603–618. https://doi.org/10.5194/gmd-8-603-2015

Kim J, Waliser DE, Mattmann CA, Goodale CE, Hart AF, Zimdars PA, Crichton DJ, Jones C, Nikulin G, Hewitson B, Jack C, Lennard C, Favre A (2014) Evaluation of the CORDEX-Africa multi-RCM hindcast: systematic model errors. Clim Dyn 42:1189–1202

Kingumbi A, Bargaoui Z, Hubert P (2009) Investigation of the rainfall variability in central Tunisia/Investigations sur la variabilité pluviométrique en Tunisie centrale. Hydr Sci J 50:3–508. https://doi.org/10.1623/hysj.50.3.493.65027

Kotlarski S, Keuler K, Christensen OB et al (2014) Regional climate modeling on European scales: a joint standard evaluation of the EURO-CORDEX RCM ensemble. Geosci Model Dev 7:1297–1333. https://doi.org/10.5194/gmd-7-1297-2014

Kupiainen M, Samuelsson P, Jones C, Jansson C, Willén U, Hansson U, Ullerstig A, Wang S, Döscher R (2011) Rossby Centre regional atmospheric model, RCA4. https://www.smhi.se/en/research/research-departments/climate-research-rossby-centre2-552/rossby-centre-regional-atmospheric-model-rca4-1.16562

Laprise R, Kornic D, Rapaic M et al (2012) Considerations of domain size and large-scale driving for nested regional climate models: impact on internal variability and ability at developing small-scale details. In: Berger A, Mesinger F, Sijacki D (eds) Climate change. Springer, Vienna. https://doi.org/10.1007/978-3-7091-0973-1_14

Leduc M, Laprise R (2009) Regional climate model sensitivity to domain size. Clim Dyn 32:833–854

Li J, Heap AD (2011) A review of comparative studies of spatial interpolation methods in environmental sciences: performance and impact factors. Ecol Inf 6:228–241. https://doi.org/10.1016/Jecoinf.2010.12.003

Lionello P, Gacic M, Gomis D, Garcia-Herrera R, Giorgi F, Planton S, Trigo R, Theocharis A, Tsimplis MN, Ulbrich U, Xoplaki E (2012) Program focuses on climate of the Mediterranean region Eos Trans. AGU 93:105–106

Llyod CD (2010) Nonstationary models for exploring and mapping monthly precipitation in the United Kingdom. Int J Climatol 30:390–405. https://doi.org/10.1002/joc.1892

Lucas-Picher P, Caya D, De Elia R, Laprise R (2008) Investigation of regional climate models' internal variability with a ten member ensemble of 10-year simulations over a large domain. Clim Dyn 31:927–940. https://doi.org/10.1007/s00382-008-0384-8

Matsumura S, Huang G, Xie S-P, Yamazaki K (2010) SST-forced and internal variability of the atmosphere in an ensemble GCM simulation. J Meteor Soc Japan 88:43–62

Matsuura K, Willmott CJ (2012) Terrestrial precipitation: 1900–2010 gridded monthly time series (version 3.02). http://climate.geog.udel.edu/~climate/html_pages/Global2011/Precip_revised_3.02/README.GlobalTsP2011.html

Meijgaard E van, Van Ulft LH, Lenderink G, de Roode SR, Wipfler L, Boers R, Timmermans RMA (2012) Refinement and application of a regional atmospheric model for climate scenario calculations of Western Europe. Climate changes Spatial Planning publication: KvR 054/12, ISBN/EAN 978-90-8815-046-3$4 pp 44

Mlawer E, Taubman S, Brown P, Iacono M, Clough S (1997) Radiative transfer for inhomogeneous atmosphere: RRTM, a validated correlated-k model for the long-wave. J Geophys Res 102:16663–16682

Nikulin G, Jones C, Giorgi F et al (2012) Precipitation climatology in an ensemble of CORDEX-Africa regional climate simulations. J Clim 25:6057–6078

Ouachani R, Bargaoui Z, Ouarda T (2013) Power of teleconnection patterns on precipitation and streamflow variability of upper Medjerda Basin. Int J Climtol 33:58–76. https://doi.org/10.1002/joc.3407

Paeth H, Born K, Podzun R, Jacob D (2005) Regional dynamical downscaling over West Africa: Model evaluation and comparison of wet and dry years. Meteorol Z 14:349–367

Panthou G, Vrac M, Drobinski P, Bastin S, Li L (2016) Impact of model resolution and Mediterranean sea coupling on hydrometeorological extremes in RCMs in the frame of HyMeX and MED-CORDEX. Clim Dyn. https://doi.org/10.1007/s00382-016-3374-2

Patricola CM, Cook KH (2010) Northern African climate at theend of the twenty-first century: an integrated application of regional and global climate models. Clim Dyn 35:193–212. https://doi.org/10.1007/s00382-009-0623-7

Pohl B, Rouault M, Sen Roy S (2014) Simulation of the annual and diurnal cycles of rainfall over South Africa by a regional climate model. Clim Dyn 43:2207–2226. https://doi.org/10.1007/s00382-013-2046-8

Price C, Federmesser B (2006) Lightning rainfall relationships in Mediterranean winter thunderstorms. Geophys Res Lett 33:L07813. https://doi.org/10.1029/2005GL024794

Raju PVS, Potty J, Mohanty UC (2001) Sensitivity of physical parameterizations on prediction of tropical cyclone Nargis over the Bay of Bengal using WRF model. Meteorol Atmos Phys 113–125.https://doi.org/10.1007/s007030110151y

Ramarohetra J, Pohl B, Sultan B (2015) Errors and uncertainties introduced by a regional climate model in climate impact assessments: example of crop yield simulations in West Africa. Environ Res Lett 10:124014. https://doi.org/10.1088/1748-9326/10/12/124014

Rinke A, Marbaix P, Dethloff k (2004) Internal variability in Arctic regional climate simulations: case study for the Sheba year. Climate Res 27:197–209

Rockel B, Will A, Hense A (ed) (2008) Special issue regional climate modelling with COSMO-CLM (CCLM). Meteorologische Zeitschrift 17(4):347–348

Ruti PM, Somot S, Giorgi F, Dubois C et al (2016) MED-CORDEX initiative for Mediterranean Climate studies. BAMS 97(7):1187–1208. https://doi.org/10.1175/BAMS-D-14-00176.1

Sanchez-Gomez E, Somot S (2016) Impact of the internal variability on the cyclone tracks simulated by a regional climate model over the Med-CORDEX domain. Clim Dyn. https://doi.org/10.1007/s00382-016-3394-y

Schneider U, Becker A, Finger P, Meyer-Christoffer A, Ziese M, Rudolf B (2013) GPCC's new land surface precipitation climatology based on quality-controlled in situ data and its role in quantifying the global water cycle. Theor Appl Climatol. https://doi.org/10.1007/s00704-013-0860-x

Sieck K, Claussen M, Jacob D (2013) Internal variability in the regional climate model REMO, vol 148. Max Planck Institute for Meteorology Rep on Earth System Science, p 129. http://pubman.mpdl.mpg.de/pubman/item/escidoc:2049540/component/escidoc:2049539/WEB_BzE_142.pdf

Simmons A, Uppala S, Dee D, Kobayashi S (2007) ERA-Interim: New ECMWF reanalysis products from 1989 onwards. ECMWF Newslett 110 25–35

Skamarock WC, Klemp JB, Dudhia J, Gill DO, Barker DM, Duda M, Huang X-Y, Wang W, Powers JG (2008) A Description of the Advanced Research WRF Version 3. NCAR Technical Note, NCAR/TN–475 + STR, p 125

Slimani M, Cudennec C, Feki H (2007) Structure du gradient pluviométrique de la transition Méditerranée–Sahara en Tunisie: déterminants géographiques et saisonnalité /Structure of the rainfall gradient in the Mediterranean–Sahara transition in Tunisia: geographical determinants and seasonality. Hydrol Sci J 52(6):1088–1102. https://doi.org/10.1623/hysJ52.6.1088

Syed et al :, Waheed I, Syed AAB, Rasul G (2014) Syed FS. (2014) Uncertainties in regional climate models simulations of South-Asian summer monsoon and climate change. Clim Dyn 42:2079–2097. https://doi.org/10.1007/s00382-013-1963-x

Sylla MB, Gaye AT, Pal JS, Jenkins GS, Bi XQ (2009) High resolution simulations of West African climate using regional climate model (RegCM3) with different lateral boundary conditions. Theor Appl Climatol 98:293–314

Tait A, Henderson R, Turner R, Zheng X (2006) Thin plate smoothing spline interpolation of daily rainfall for New Zealand using a climatological rainfall surface. Int J Climatol 26:2097–2115. https://doi.org/10.1002/joc.1350

Tebaldi C, Knutti R (2007) The use of the multi-model ensemble in probabilistic climate projections. Phil Trans R Soc A 365:2053–2075. https://doi.org/10.1098/rsta.2007.2076

Vaittinada Ayar P, Vrac M, Bastin S, Carreau J, Déqué M, Gallardo C (2016) Intercomparison of statistical and dynamical downscaling models under the EURO- and MED-CORDEX initiative framework: present climate evaluations. Clim Dyn 46:1301–1329. https://doi.org/10.1007/s00382-015-2647-5

Vautard R, Gobiet A, Jacob D et al (2013) The simulation of European heat waves from an ensemble of regional climate models within the EURO-CORDEX project. Clim Dyn 41:2555–2575. https://doi.org/10.1007/s00382-013-1714-z

Verner D (2013) Tunisia in a Changing Climate: Assessment and Actions for Increased Resilience and Development. Washington, DC: World Bank. © World Bank. https://openknowledge.worldbank.org/handle/10986/13114 **(License: CC BY 3.0 IGO)**

Warrach-Sagi K, Schwitalla T, Wulfmeyer V, Bauer H-S (2013) Evaluation of a climate simulation in Europe based on the WRF–NOAH model system: precipitation in Germany. Clim Dyn 41:755–774. https://doi.org/10.1007/s00382-013-1727-7

Wu W, Lynch AH, Rivers A (2005) Estimating the uncertainty in a regional climate model related to initial and boundary conditions. J Clim 18:917–933

Wu C-C, Zhan R, Lu Y, Wang Y (2012) Internal variability of the dynamically downscaled tropical cyclone activity over the western North Pacific by the IPRC Regional Atmospheric Model. J Clim 25(6):2104–2122

Xoplaki E, Gonzalez-Rouco JF, Luterbacher J (2003) Mediterranean summer air temperature variability and its connection to the large-scale atmospheric circulation and SSTs. Clim Dyn 20:723–739. https://doi.org/10.1007/s00382-003-0304-x